Development of a smart biodiagnostic platform for point of care detection by multiplexed electrokinetic sensing

A Dissertation Presented for the

Doctor of Philosophy

Degree

University of Tennessee, Knoxville

Rania Oueslati

December 2019

To my hard-working parents who have sacrificed their lives for me.

To my husband Walid Mathlouthi who provided unconditional love and care.

Acknowledgments

The work presented in this dissertation would not be possible without the contributions of many individuals, and I can only hope to mention some of the most important here.

I would like to first express my special thanks of gratitude to Dr. Jie (Jayne) Wu, my Ph.D. advisor, for her professional guidance. Her mentorship helped me overcome many obstacles one after another throughout my entire graduate study. This work would not have been possible without what I have learnt from her.

I would like to thank Dr. Benjamin J. Blalock, Dr. Gong Gu and Dr. Anming Hu for serving as the committee members. Each of the members of my Dissertation Committee has provided me extensive personal and professional guidance and taught me a great deal about both scientific research and life in general. Their meaningful suggestions make my research a more solid and comprehensive work.

I would like to express my special thanks to the University of Tennessee Initiative for PON/POC Nanobiosensing, and the US DHS for providing me the opportunity for further improvement and perfection of my work.

Last but not least, Nobody has been more important to me in the pursuit of this project than the members of my family. I would like to thank my Mom and Dad, whose love and guidance are wit me in whatever I pursue. They are the ultimate role models. Most importantly, I wish to thank my loving and supportive Husband, Walid , my four beloved sister and my wonderful brother, Ichrak, Asma, Amal, Rahma and Ahmed Amine who provide unending inspiration.

Abstract

Pathogenic infections, foodborne illnesses and drug abuse pose significant public health issues worldwide, and they are of special concern in developing countries, where the medical resources and public hygiene are limited. Therefore, rapid detection and identification of these pathogens are of paramount importance for adopting treatment options and to establish adequate control measures. The detection and recognition of these bacterial microorganisms still rely on complex methods, which maybe not be adequate for point of care detection. Therefore, a great research challenge in this field is focused to develop fast, accurate, selective, and sensitive protocols to detect these bacteria at low cost. Also, the lab-on-chip development for large scale screening analysis demands improved miniaturization, reduction of processing time and cost, and multianalyte detection. In addition, simultaneous monitoring of multiple molecular interactions and multiplexed detection of multiple diagnostic biomarkers at very low concentrations have become important matters in advanced biomedical and electrochemical sensing. This work presents the design of a portable system for sensitive and quantitative detection of DNA and drug biomarkers which will be highly valuable in controlling and preventing disease outbreaks. First, this work investigates the development of assay protocols for highly sensitive and selective on-site detection of Drugs and bacterial DNA. This is an improvement over the priorily developed AC electrokinetics-based capacitive sensing, which is capable of detecting specific target in a point-of-care setting using micro-fabricated interdigitated electrodes. Second, this work presents the development of a smart bio-diagnostic platform for point of care detection to interface with capacitive electrokinetic electrodes for a multiplexed sensing. The circuit has shown good accuracy on various test devices. In association with the ACEK capacitive sensing, preliminary data are collected and successfully used to characterize physiological samples (10μl).

Table of Contents

List of Tables

List of Figures

Chapter 1

Introduction

1.1 Motivation

Pathogenic infections and associated foodborne illnesses pose signicant public health issues worldwide, and they are of special concern in developing countries, where the medical resources and public hygiene are limited. In fact, the increase in the number of bacterial strains that show resistance to methicillin has become a serious clinical and epidemiological problem because this antibiotic is considered as the first option in the treatment of staphylococci infections, and because resistance to this antibiotic implies resistance to all B-lactam antibiotics[5]. Methicillin-resistant Staphylococcus aureus (MRSA) is one of the most prevalent causes of nosocomial and community-acquired infections with poor clinic consequences[6, 7]. Patients with MRSA infection without timely treatment face significantly higher mortality and morbidity rates than patients infected with methicillin-susceptible S.aureus. Therefore, fast and reliable methods for detection of MRSA are warranted to limit the spread of infection. Drug abuse as well, has been declared a public health emergency of international concern as it contributes to severe social problems. Cocaine, also known as benzoylmethylecgonine, is a strong stimulant used mostly as an illegal recreational drug [8]. This psychostimulant has become a noticeable part of the worldwide drug scene.According to World Health Organization (WHO), the US is an outlier in cocaine use as 16 % of adults have used this drug [9]. Hence, drug abuse is becoming a serious global public health problem and a contributing factor to severe somatic, cognitive and psychological complications.

In the face of such a harsh reality, there is a need for reliable, simple to use and low cost devices which can detect and identify different microorganism species at low cost. These testing methods can be sought after for on-site illegal drug screening by law enforcement or in numerous fields such as clinical diagnostics, environmental monitoring, and food quality controlling. Therefore, the rapid detection and identication of these pathogens are of paramount importance for adopting treatment options and to establish adequate control measures.

Biosensors have shown great potential in realizing on-site diagnosis. Biosensors are defined as analytical devices incorporating biological or biological-derived sensing elements either integrated within or intimately associated with physicochemical transducers for analyte detections[10, 11, 12]. Over past decades, various biologically derived materials, such as nucleic acid, bacteria, and aptamers, have been incorporated to fabricate biosensors with high performances[13, 14, 15, 16]. They are of considerable interest due to their tremendous promise for detecting and identifying micro in a faster, simpler and cheaper manner compared to traditional hybridization assays.

1.2 Affinity Biosensor: Performances and Challenges

A biosensor is a device designed to detect or quantify a biochemical molecule such as a particular DNA sequence or particular protein. Many biosensors are affinity-based meaning they detect the occurrence of specific biomolecular affinity reactions, such as antigen-antibody binding or DNA-DNA hybridization[17]. As represented in the term itself, affinity-based bio-sensing is based on two fundamental steps. The first one, called affinity step, is binding the desired target while excluding non-target binding. The second step, the readout step, is detecting a change in the surface properties. The affinity step is based on the surface chemistry and biological binding, while the readout step is based on the physics of detection with associated signal processing[18]. Based on signal transduction, biosensors can be classified as optical and electrochemical sensors. Optical sensors (e.g. fluorescence, surface plasmon resonance (SPR) and chemiluminescence), transduce the bio-molecular interaction into an optical signal, such as a change in light intensity. Electrochemical biosensors which

are mainly categorized into three types (amperometric or potentiometric and Impedimetric), rely solely on the measurement of currents and/or voltages to detect binding[19, 20, 21]. Amperometric sensing, as the name implies, is realized through the measurement of the current at a fixed potential. This technique is called potentiostatic detection. The measured parameter in potentiometric sensing is either the change on the surface charge or potential charge. In fact, if the probe and the analyte bind together the interface of the sensor, the net charge density will change compared with that of the probe alone, which can be measured by a potentiometer. A reference electrode in the same solution is set at a constant potential as a reference. Aside from the change of net charge, the potentiometric signal can also be generated by changes in the pH or redox state. Potentiometric sensors can be ion-selective electrodes (ISE) or field effect transistor (FET). Concerning impedimetric biosensors, an alternating current (AC) signal is applied between a pair of working electrodes. If an interaction occurs between the analyte and the immobilized probe, the impedance of the electrode will change. This variation can be measured by an impedance analyzer.

To sum up, Affinity biosensors are classified based on different types of transducers. A desired biosensor most commonly possesses general characteristics such as real-time monitoring, sensitivity and selectivity which will open up new opportunities for Point of Care (POC) diagnosis. The deployment of these devices in the field would provide a low-cost and rapid detection tool of diseases.

1.3 Scope and Research Goal

To build a fully qualified technology for POC diagnosis in real world, the feasibility of biosensors needs further improvement. Thus, both affinity and readout steps need to be improved. Arguably, the most daunting issues for POC diagnostics are sensitivity, selectivity and response time. Although many publications claim to be able to detect infectious diseases at very low levels[22, 23], most of them are determined in the absence of non-target interference, involve strict samples treatment and long processing time. Since it is rare for such clean samples to be realistic in practical applications, reported limits of detection might be misleading in determining a biosensors real-world performance[24]. In real world

detection, biosensors should be challenged with mixed target/non-target analytes to verify its feasibility. Hence, obtaining adequate selectivity in complex samples such as blood serum or saliva is another major challenge that has to be overcome before any practical use of biosensors. Moreover, affinity biosensors need a long time to yield result, which limits the applicability of these tests for many clinical conditions. The obstacle to achieving rapid detection is the long diffusion time for the target bio-particles to reach the sensing site of a sensor. So accelerating the diffusion process has been an essential part of our design. On the other hand, one major thrust for bio-sensing research is to achieve effective multiplex detection in the clinic or at the bedside. Simultaneous monitoring of multiplexed sensing and on-site detection of several diagnostic bio-markers at very low concentrations remains as one of the top challenges for POC diagnosis.

In this work, a low cost and portable analyzer with good accuracy is designed for a true POC technology. An alternating current electrokinetic (ACEK) effects including dielectrophoresis (DEP) and AC electroosmosis (ACEO)[3] have been used to improve the sensor sensitivity and response time by accelerating the travel of target molecules to the electrode surface[25, 26]. Also, a portable system for sensitive and quantitative detection compatible with large molecules (DNA) and small biomarkers (drug) is designed for field use to control and prevent diseases outbreaks.

1.4 Synopsis

This report is organized as follows.

Chapter 2 reviews the latest development of biosensors and bioelectronics for biochemical detection and introduces future perspectives to improve POC sensing.

Chapter 3 introduces the basics of ACEK capacitive sensing and explains the theory of electrochemical impedance spectroscopy. The design and characterization of sensing devices is also discussed.

Chapter 4 describes the concept of incorporating capacitive sensing to detect specific targets (drugs and DNA). Afterwards, improvement of sensor performance is discussed.

Chapter 5 first presents the Overview of the readout operation then describes in details the development of AC-electrokinectic-Based capactive (ABC) readout.

Chapter 6 presents experimental results which are used to evaluate the ABC multiplexed bio-sensing.

Finally, the work is summarized and future work are proposed in Chapter 7.

Chapter 2

The State of Art

The clear and enormous need for healthcare and environmental monitoring continues to drive substantial research in the field of biosensor. To address the challenge, numerous research effort have been dedicated to improve the laboratory based biosensing assays. Other researchers have attempted to integrate portable into biosensors and bioelectronics to reduce the overall size and cost of the transducing systems.

This chapter briefly discusses the research relating to drugs and DNA detection and sheds lights on the instrumentation required for electrochemical impedance spectroscopy. Majority of the embedded sensors cited in this chapter used the chip AD5933 (High performance Impedance Converter Network) from Analog Devices to measure the sensor impedance. This chapter also highlights the contribution done in this work.

2.1 Literature survey

2.1.1 Laboratory-based biosensors for Drug and DNA detection

Aptasensors for cocaine detection

Conventional methods for cocaine detection are mostly mass spectrometry-based analytical techniques or high pressure liquid chromatography assays coupled with various detection methods such as UVabsorbance or fluorescence[27, 28, 29]. These methods have limits of detection (LOD) around nanomolar (nM) level, and they are often associated with

shortcomings such as being time consuming, high cost, requires skilled personnel and complicated sample preparation[30]. Hence, there is an unmet need for the development of an easy and low cost method for on-site cocaine detection in complex biological fluids. Recently, aptamer-based biosensors (also known as aptasensors) have received considerable attention for cocaine detection[31, 32, 33]. Aptamers are single-strand DNA or RNA oligonucleotides, and recognize specific targets owing to hydrogen bonding, electrostatic or hydrophobic interactions, etc.[34]. Due to their high sensitivity, low cross-reactivity to small molecules and high stability, they are gaining popularity as a probe for biosensors based on specific binding. Several types of aptasensors have been reported for cocaine detection. Qiu et al. used a hairpin-probe and isothermal circular strand-displacement amplification to increase the response of the cocaine capture probes. This method shows a LOD of 190 nM. Zhang et al. develop a colorimetric aptasensor using gold nanoparticles (AuNPs) for cocaine detection as low as 2 M in NaCl solution[33]. In a chemiluminescence aptasensor,Au-NPs has been used to improve the LOD of cocaine detection to nM level in phosphate-buffered saline (PBS) [35]. In addition to the aforementioned optical methods, aptasensors can also be adapted for electrochemical detection. Zhang et al. [33] develop an aptasensor based on the formation of a supramolecular aptamer fragments/cocaine complex with an LOD of 0.1 μM. Two fragments of anti-cocaine aptamer self-assembled into a supra molecular cocaineaptamer fragments complex only in the presence of cocaine molecule. The cocaine is detected by the change of the electron transfer resistance, which are strongly correlated to cocaine concentration in PBS. Jiang et al. demonstrate a cocaine sensor using two engineered aptamers in connection to redox-recycling signal amplification[28]. The electron transfers are enhanced by electrochemically depositing graphene/AuNP nanocomposites on a screen printed carbon electrode. The presence of the target cocaine and subsequently added biotin-modified secondary binding aptamers would form sandwich complexes on the electrode surface. The LOD of this assay are 1 nM cocaine. The aforementioned electrochemical-based aptasensors, although cheap and easy to implement, do require labeling which would make the detection process complicated and long, and might affect the bio-affinity between the aptamers and the target cocaine molecules[25].

Bio-detection of MRSA infection

In recent years, the increase in the number of bacterial strains that show resistance to methicillin has become a serious clinical and epidemiological problem because this antibiotic is considered as the first option in the treatment of staphylococci infections, and because resistance to this antibiotic implies resistance to all β-lactam antibiotics[5]. Methicillin-resistant Staphylococcus aureus (MRSA) is one of the most prevalent causes of nosocomial and community-acquired infections with worst clinic consequences[6, 7]. Patients with MRSA infection without timely treatment face significantly higher mortality and morbidity rates than patients infected with methicillin-susceptible S aureus. Therefore, fast and reliable methods for detection of MRSA are warranted to limit the spread of infection.

To control the spread of MRSA, culture methods including pulsed-field gel electrophoresis (PFGE), multilocus sequence typing (MLST), spa typing, and SCCmec typing[36] have been reported as conventional approaches for MRSA detection. These methods are useful for typing and monitoring different strains of MRSA and studying their evolution. Typically, they involve the growth of microorganisms on plates with predetermined culture medium under controlled conditions that allows the specific bacteria to multiply for subsequent colony enumeration. Detection of MRSA by culture methods offers high sensitivity but they are expensive, laborious and time consuming [37].

Molecular diagnostics, as another conventional method for MRSA detection, target nucleic acids from microorganisms of interest. In fact, resistance to methicillin is mediated by the presence of penicillin-binding protein 2a (PBP-2a), encoded by the mecA gene, located in the staphylococcal cassette chromosome mec (SCCmec)[38]. Extensive variation of the SCCmec structural organization and genetic content may exist among MRSA isolates, however, the sequence of the mecA gene is highly conserved. It is therefore possible to accurately detect/differentiate Staphylococcal species based on their genetic information[39].

Several methods for molecular detection of the mecA gene,using DNA microarrays, have been reported recently[40, 41, 42]. Tombelli et al. develop piezoelectric biosensor using gold electrodes. It is applied to the analysis of DNA samples extracted from bacterial DNA and amplified by polymerase chain reaction(PCR). Two immobilization methods

and denaturation protocols are used to study the influences of these parameters on the performances of the sensor and applied to the detection of the mecA gene. This method shows a dynamic range of 0.06 $\rightarrow$ 0.75μM of MRSA DNA samples.[43]. Corrigan et al. used electrochemical impedance spectroscopy (EIS) in combination with a PCR step to demonstrate the detection of the antibiotic resistance gene mecA. This method shows a limit of detection for 10 pM of mrsa DNA using screen printed electrodes.[39]

2.1.2 Impedance-based nanobiosensors on portable sensing systems

On-site or point-of-care detection of drugs and infectious diseases has unmet needs of finding a rapid, sensitive, specific and simple-to-use sensing method. Rapid, sensitive and reliable detection of specific target is critical to diagnose and differentiate drugs and bacterial diseases. To be viable as a POC diagnostic system,a readout platform which needs to be portable, embedded, and user friendly is needed to provide low cost and fast analysis of patient samples. Recently, researchers have been working on microtechnology to develop biosensors for on-site detection.

Currently, much work has focused on miniaturization and optimization of these bioelectronics devices, such as micro-fabricated transducers and compact readout instruments, to achieve real-time, point-of-care, and easy-to-use detection for analytes , especially for clinic and environmental samples [44, 45, 46].

While gaining improvements in sensitivity and automation, most of micro/nano-biosensors still require cumbersome readout instruments to detect response signals, analyze data, and display results. Sometimes, the instruments become even more complicated in design and larger in size because of other extra components, such as valves and pumps for microfluidics, to use in coordination with nano-sensors [47, 48, 49]. Thus, bulkiness and overall cost of the readout devices became new obstacles following miniaturization of biosensors for portable and cost-effective detection.

Optical methods such as surface enhanced Raman scattering and surface plasmon resonance are often associate with shortcomings such as being time consuming, high cost,

requires skilled personnel and complex sample preparation. Acoustic wave sensors and colorimetric assays are easily liable to interfere with the changes in the environment and fluid properties.On the other hand, Electrochemical and EIS sensing are low cost and easy methods to implement, well suited for on-site detection with limited resources [50]. It shows broad applications of quantitative detection for important analytes (e.g., proteins, metabolites, nucleic acids, and metal ions) over past decades [51, 52, 53].

In the electrochemical impedance spectroscopy (EIS) system, several portable impedance-based sensing systems have been developed. But few of them can meet the needs of ACEK capacitive sensing. Among the reported work, Jian et al[1] develop an electrochemical impedance spectroscopic biosensor to detect E.coli bacteria using a smart-phone.They sweep frequency from 2 to 100 kHz to measure the E.coli sensor impedance. They use Arduino microprocessor board to control the AD 5933 chip to send sinusoidal signals to the bacteria sensor. The response signal is sent back to the smartphone through the Bluetooth and the impedance value with respect to frequency will then be plotted on the screen. Similarly, Zhang et al.[54] use impedance spectroscopy with screen printed electrodes, to report the 2,4,6-trinitrotoluene(TNT) detection in PBS. By applying a 200 mV AC voltage with a 1 V DC bias and a frequency range from 10 Hz to 10 kHz, the impedance change caused by the binding of TNT to special peptides on the electrodes is recorded by a handheld device and sent out to smartphone through Bluetooth. Despite their good sensitivity and accuracy, the aforementioned devices can not work without the smartphone which increase the price of the reader and limit the user to use a phone. More importantly, the output voltage of EIS is supplied from the chip AD5933. This excitation signal can be one of the four DC biased AC ranges. This biasing can harm the biosensor and lead to an impedance misread. Other than using AD5933, integrated chips (ICs) have been used to custom-design impedance detection system [55, 56].Chuang et al,[55] attempted to control the highly accurate impedance analyzer, AD5933, and to construct a wireless communication architecture based on the Zigbee chip. To measure the impedance, their group uses the commercial AD5933 to initiate the stimulus signal, sample the response signal and calculate the impedance of the sensor.

Afterwards, using the LabVIEW based platform, the measurement system achieves the far-end control and computation system in the PC, which can complete the final frequency response. The use of the LabVIEW interface on a PC impede POC diagnosis.

Jian et al [1] present in their work a module-level impedance measurement system integrated with a disposable electrode for the immunoassay of bladder cancer cell lysate (T24) to a specific antibody (galectin-1). In 10 min, their sensor detects 0.0626 mg/ml of cell lysate. Their proposed system module (as shown in figure 2.1) integrates three modules: impedance analyzer platform, microcontroller unit (MCU) and wireless communication. The impedance magnitude is the only parameter used to detect the specific binding in this test. The phase change and the impedance introduced by the soldered components in the signal path of the readout system is not reported. Table 2.1 summarizes and compare the portable electrical biosensors reported recently.

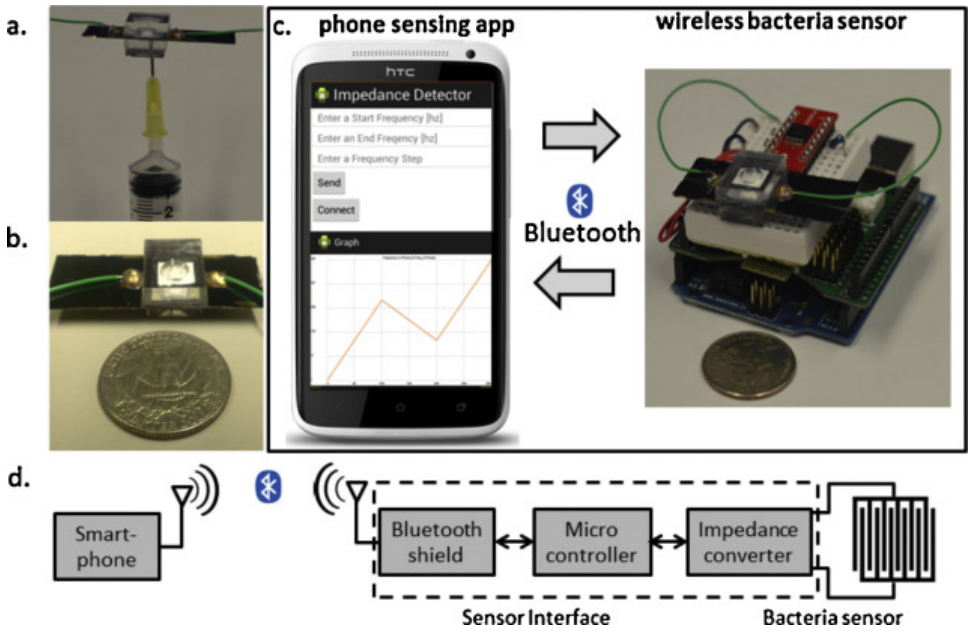

Figure 2.1: Wireless mobile phone bacteria sensing system. (a) Picture showing syringe injection of testing liquid into the sensor package; (b) close view of the EIS bacteria sensor package; (c) picture showing communication scheme between smartphone sensing app and wireless bacteria sensor; (d) diagram of wireless sensing system.,adapted from [1], Copyright 2014.

Table 2.1: Specifications of embedded impedance-based readout systems in the literature

Analyte	Excitation signal	Frequency	Sensitivity-LOD	Reference
E.coli	NA	1 kHz to 1 MHz	$10^1 to 10^4$ CFU/mL	[1]
Bull serum albumin(BSA)	200 mV, DC bias 1 V	10 Hz to 10 kHz	1.78 μg/mL	[54]
Cell lysate	10Vpp	50Khz	62.6μg/mL	[55]
TNT	200 mV	10 kHz to 100 kHz	$10^{-6} to 10^{-3}$ M	[57]
DNA(MRSA) Drug(Cocaine)	20mVpp to 2Vpp	1kHz to 100 kHz	3.15 MRSA copies/μL 7 fM of cocaine in Human serum	This work

2.2 Contribution

The main contributions of this work include

- The development of Cocaine aptasensor using capacitive monitoring of sensor surface incorporating alternating current electrokinetics effects to speed up molecular transport and minimize matrix effects. The aptasensor is rapid, low cost, highly sensitive and specific as well as simple-to-use for the detection of cocaine from serum. The assay has a sample-to-result time of 30s, a limit of detection of 7.8 fM, and a linear response for cocaine ranging from 14.5fM to 14.5pM in standard buffer, which are great improvements from other reported cocaine sensors.

- The development of an electrochemical sensor called AC electrokinetics-based capacitive (ABC) biosensor, for the detection of genomic DNA (gDNA) of methicillin-resistant Staphylococcus aureus (MRSA). After optimization of nano-structured sensor surface and signal processing, the ABC sensor demonstrates fast turnaround of results (10 s detection), excellent sensitivity (a detection limit of 4.7 DNA copies /L MRSA gDNA) and high specificity, suitable for point of care diagnosis.

- Design of an embedded capacitance acquisition platform that meets the requirements of ACEK capacitive sensing, i.e. from 1kHz to 100 kHz and zero-DC biased AC signal with wide amplitude range (10 mV $\rightarrow$ 2 Vpp) to induce ACEK eects. The designed board is suitable for DNA and drug detection.

- Reduction of the measurement embedded readout system size from a benchtop size box to a palm size board.

- Real time multiplexed detection of different targets.

Chapter 3

Sensing mechanism and sensor structure

3.1 Interfacial capacitance sensing

ACEK capacitive sensing method adopts IDEs as its sensor, which consists of a series of parallel microband electrodes with alternating microbands connected to a common pad. The IDEs are functionalized with probe molecule to achieve detection specificity. Only target molecules are expected to bind with probe molecules immobilized on the IDE surface. The binding events are detected by tracking the capacitance change at the interface between the electrode and sample solution. This method has been used to detect small molecules, proteins, virus particles, and nuclei acids [58, 59, 60, 61].

When electrodes are immersed in electrolytes, the resultant system can be represented as a network of surface and bulk components, both with capacitive and resistive elements [62, 3]. For an AC frequency range below several hundred kHz (kiloHertz), the electric network can be further simplified as a serial connection of interfacial capacitance Cint and bulk resistance Rf [63, 64] as shown in Figure 3.1 .

As schematically shown in Figure 3.2, binding of cocaine molecules with the immobilized aptamer causes an increase in the thickness of the dielectric layer at the IDE surface. Before

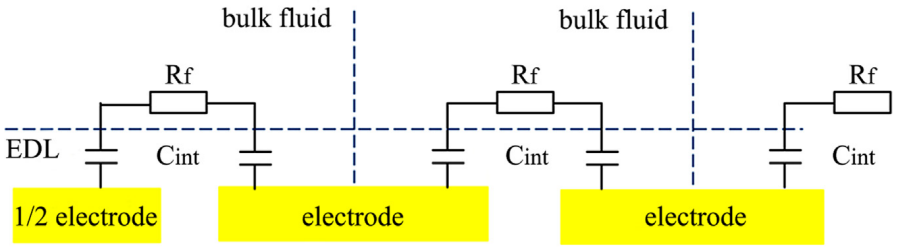

Figure 3.1: The simplified equivalent circuit of electrolyte/electrode system.

surface functionalization, the bare electrode exhibits an interfacial capacitance due to the formation of electrical double layer (EDL) with a Debye length of λ edl, which is electrically equivalent to having a dielectric layer with a thickness of λ edl (3.2(a)) between two parallel electrode plates. After the immobilization of the aptamer and the blocking molecules on the surface (3.2(b)), another layer λ 0 will be added to λ edl. Then, the dielectric layer thickness becomes $\lambda edl + \lambda 0$ and the interfacial capacitance of the sensor before the binding of target molecule is expressed as:

$$C_{int,0} = \frac{A_{int}}{\frac{\lambda_0}{\epsilon_p} + \frac{\lambda_{edl}}{\epsilon_s}} \tag{3.1}$$

where A_{int} is the surface area of the interfacial capacitor of the functionalized electrode, ϵ_p is the probe molecule permittivity and ϵ_s is the double layer permittivity. When cocaine molecules bind to the immobilized probe, a third dielectric layer with a thickness c will be

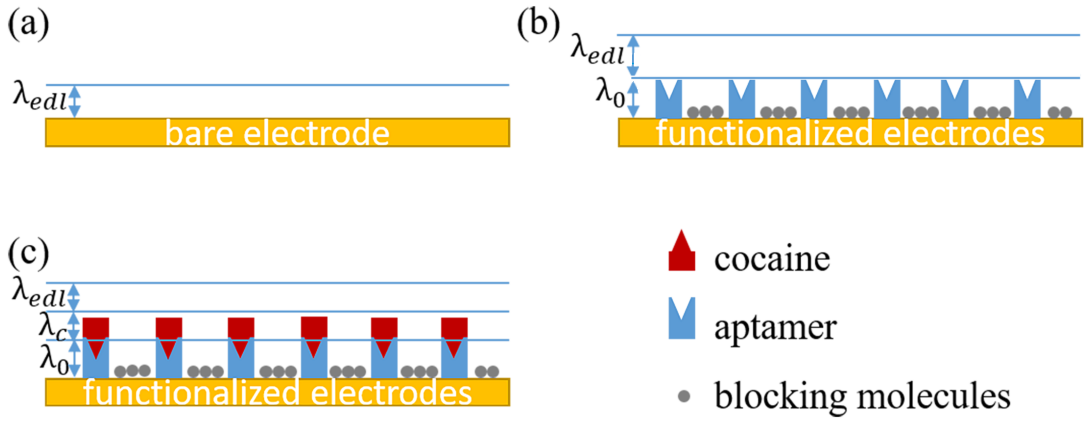

Figure 3.2: Changes in the interfacial capacitance of an electrode at different stages of sensor functionalization and cocaine binding. (a) Before functionalization, λedl is the thickness of the EDL (b) After immobilization of the aptamer, and the thickness of interfacial dielectrics becomes $\lambda edl + \lambda 0$. (c) Cocaine molecules bind to the immobilized aptamer and the dielectric thickness increases by λc, which causes a decrease in the interfacial capacitance value.

added to λ_{edl} and λ_0 (Figure 1(c)). The interfacial capacitance expression becomes:

$$C_{int,1} = \frac{A_{int,co}}{\frac{\lambda_0+\lambda_c}{\epsilon_p} + \frac{\lambda_{edl}}{\epsilon_s}} \tag{3.2}$$

Based on equations 3.1 and 3.2, the binding of Cocaine molecules can be detected by calculating the capacitance change ratio $\frac{C_{int1}-C_{int0}}{C_{int0}}$.

By using normalized capacitance change rate, the response variation caused by the difference in microelectrode initial impedance can be minimized. The readout is also independent of the actual working area of sensors.Consequently, good test repeatability is expected of this method.

3.2 AC Electrokinetics mechanisms

ACEK effects, including dielectrophoresis (DEP), AC electroosmosis (ACEO) and AC electrothermal (ACET) effects, are increasingly used in microfluidic devices to manipulate

fluids and embedded objects[3]. DEP directly acts on the particles embedded in the fluid, while ACEO and ACET effects induce fluid movements that carry the embedded particles.

Affinity based biosensors typically relies on passive diffusion of target macromolecules to bind on the electrodess surface, which can cause a long detection time (hours or even days) and low sensitivity. [65]. To improve affinity based sensor ′s sensitivity and selectivity, great research effort has been devoted to develop an active guidance of biomolecules to direct them to sensors and shorten the detection time. The sensing mechanism adopted for our bacterium DNA detection is based on ACEK enhanced capacitive sensing. A special AC measuring signal is applied between a pair of functionalized interdigitated microelectrodes (IDMEs). ACEK effects use an AC electric field to induce particle and fluid movement [26], so that macromolecules can be in situ concentrated onto microsensors. There are three major ACEK effectsDEP, ACEO and ACET effects. With AC electric field inducing particle and fluid movement, biomolecules can be accumulated in-situ over the surface of electrodes[3]. ACEK effects improve the sensor sensitivity and response time by accelerating the travel of target molecules to the electrode surface[25, 26].

3.2.1 Target Enrichment by Dielectrophoresis (DEP)

When an non-uniform AC electric field is applied to an aqueous solution, electric field density on one side of the solutions particle will be larger than that on the other side [66], which would lead to a net force on the particle that can be induced to transport particles. This force is called a dielectrophoresis (DEP) force. This technique has been studied in great details for controlled manipulation of particles, binary separation, and characterization of particles. [67, 68]. As shown in figure 3.3, Dielectrophoresis (DEP) is an efficient particle manipulation method in microfluidics. It is based on the differences in the electrical and dielectrical properties between the medium and the embedded particles[69, 70, 71]. Based on the sizes of targets and electrode design, DEP force can be the dominant attraction/enrichment effect against other AC electrokinetic effects for the enrichment of target analytes [66].

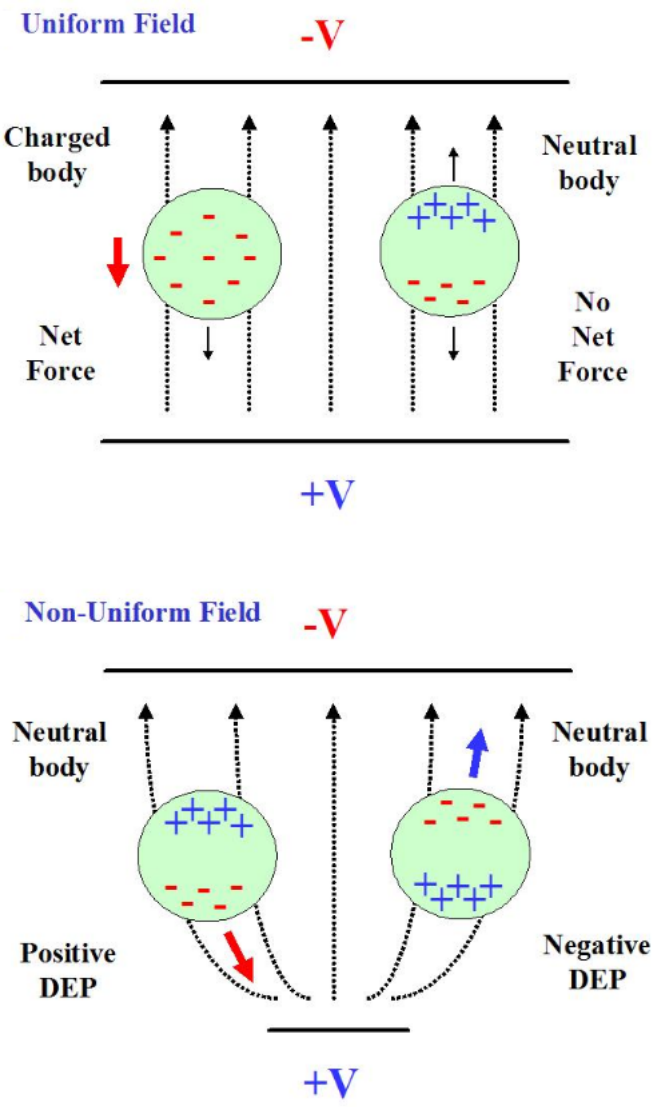

Figure 3.3: Schematic illustrating positive and negative dielectrophoresis (DEP)[2]

As in this work, our target particles can be cylindrical or spherical, the DEP velocity υ_{CylDEP} for cylindral target can be described as follows: [61],

$$\upsilon_{Cyl,DEP} = \frac{r^2 ln(\frac{2l}{r})}{18\eta} * \epsilon_m * RE[K(\omega)] * \nabla|E|^2 \tag{3.3}$$

and the DEP velocity υ_{sphDEP} for spherical target is as follows:

$$\upsilon_{sph,DEP} = \frac{ar^2}{3\eta} * \epsilon_m * RE[K(\omega)] * \nabla|E|^2 \tag{3.4}$$

where ϵ_m and η are respectively the permittivity and the viscosity of the medium, r and l are respectively the radius and the length of the target molecule cross section. $\nabla|E|^2$ is the gradient of the square of electric eld strength in root mean square (RMS) value. Re[K(ω)] is the real part of Clausius-Mossotian factor being limited between 0.5 and 1, and K(ω), as the Clausius-Mossi factor, is defined to be $K(\omega) = \frac{\epsilon_p^* - \epsilon_m^*}{\epsilon_m^*}$. $\epsilon^* = \epsilon\frac{j\sigma}{\omega}$ is the complex permittivity with ϵ, σ,and ω being permittivity, electrical conductivity and electric field angular frequency. Subscripts p and m denote particle and medium, respectively.

The real part of the Clausius-Mossotti factor determines the polarity of DEP force. When positive, the particle experiences positive DEP force, moving towards high electric field regions, such as electrode edges; whereas when negative, the particles experiences negative DEP, being repelled from electrodes. Based on equations 3.3 and 3.4, the DEP force is dependent on AC frequency and medium's ionic strength.

3.2.2 Target Enrichment by AC electroosmosis (ACEO)

ACEO effect can induce microfluidic vortices above electrodes to transport target molecules to the electrode surface for binding [72, 26], which improves the detection sensitivity and response time. ACEO typically dominates at low ionic strengths, such as target samples diluted in water. Flow velocity of ACEO has been observed to decrease significantly with increasing conductivity and eventually drop to zero above 0.085 S/m [73]. Hence for medical

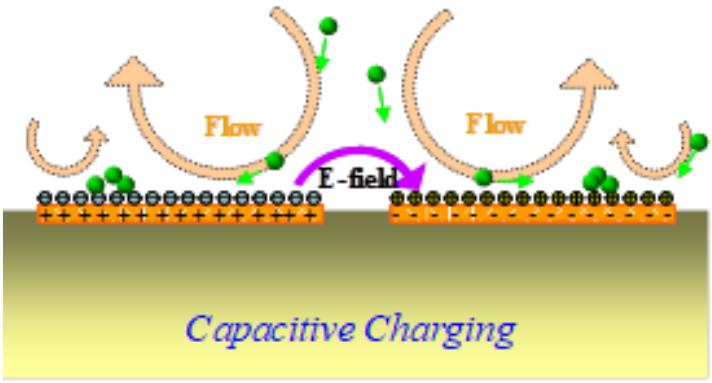

Figure 3.4: Induced electroosmotic flows over a pair of electrodes [3]

and biological applications involve the use of solution with low conductivity the ACEO flow will be dominant.

Figure 3.5 illustrates the movement of microflows in opposite directions.These ACEO flows are caused by the movement of induced charges in the EDL at the solid-liquid interface when a non-uniform AC electric field is applied. The induced counter-ions will move under a tangential electric field to generate ACEO flows.

ACEO fluid velocity is approximately given as

$$\upsilon_{ACEO} = \frac{-\epsilon_m}{\eta} * \Delta\xi * E_t \tag{3.5}$$

where ϵ_m and η are the permittivity and viscosity of the medium, E_t is the component of the electric field strength tangential to the electrode surface, and $\Delta\xi$ is the voltage drop over the interfacial layer including the EDL and molecular deposition at the electrode surface[66]. ACEO velocity is known to exhibit a bell-shaped dependence on frequency due to the charging process of EDL. Therefore, the frequency of capacitive sensing needs to be optimized to maximize ACEO effect.

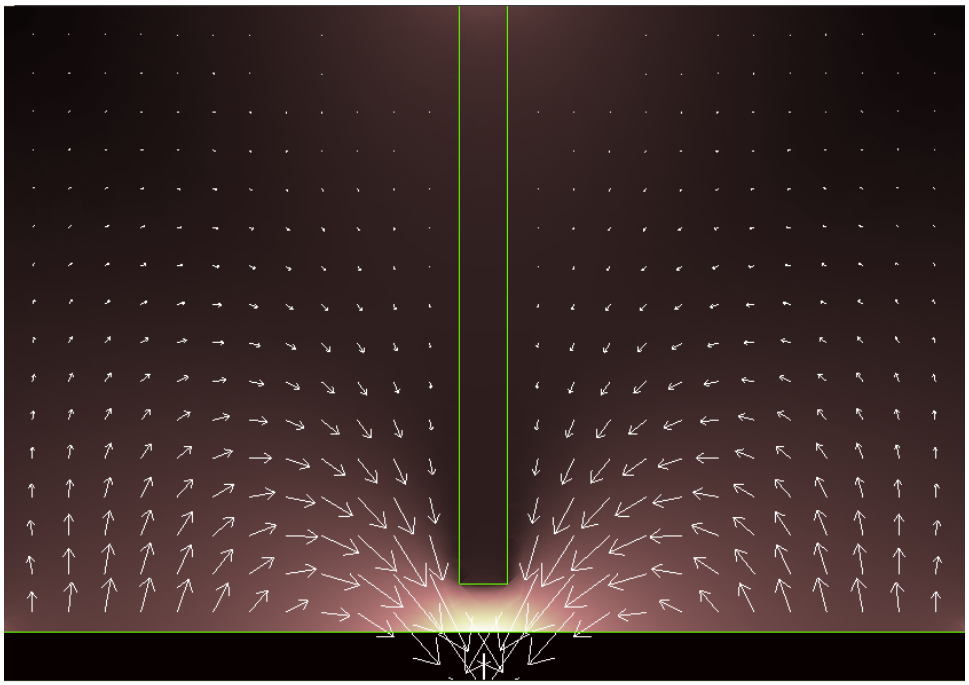

Figure 3.5: Numerical simulation of thermal gradients(color) and ACET flow field (arrows). (Light color indicates higher magnitude)[3]

3.2.3 Target Enrichment by AC electrothermal (ACET)

The ACET effect is responsible for the flow pattern at high frequencies. This effect effect arises from uneven Joule heating due to an electric current flowing through the fluid. Once the AC electric field is applied in the bulk solution, embedded molecules would migrate with the generated flow.

The time average electric thermal force is shown in Equation

$$\upsilon_{ET} \approx 5 * 10^{-4} * \frac{\epsilon_m \delta V^4}{K\eta r} * |\frac{1}{\delta}\frac{d\delta}{dT}| \tag{3.6}$$

where η is the viscosity of medium, K is thermal conductivity of mediumϵ_m is the electrical conductivity of medium. V is the applied voltage and T is the temperature.

3.3 Electrode design and surface monitoring

3.3.1 Microeelectrode sensor design

The ACEK-based capacitive affinity biosensor utilizes arrays of co-planar interdigitated microelectrodes(IDME). The detection of the studied target molecules is performed using both aluminum and gold IDMEs. Aluminum electrodes are commercially available from Qualcomm B39431R880H210 surface acoustic wave (SAW) chip. The electrode nger is 2.0 μm wide and 170 μm long. The gap between each nger is 1.5 μm. The metal cover of the SAW resonator is removed mechanically to expose the working electrode array for use, as shown in Figure 3.6. The metal housing around the electrode chip is about 4mm (L) x 2.5mm (W) x 1mm (H), and accommodates 10 μL of sample. The interdigitated electrodes are electrically connected to two contact pads on the chip bottom, which are then connected to an impedance analyzer.

Gold electrodes (shown in figure 3.7) are fabricated based on printed circuit board (PCB) technique with a simple and low cost process. The electrode digit is 400 m wide and 1 cm long with a 200 μm spacing between each. The IDMEs are electrically connected to two contact pads, which are then used to connect to the impedance analyzer. The fabrication steps are as follow: The pattern of the in-house electrodes is printed on toner transfer paper in ink and then transferred onto the copper sheet by using laminator whose temperature is set to be 379 F.

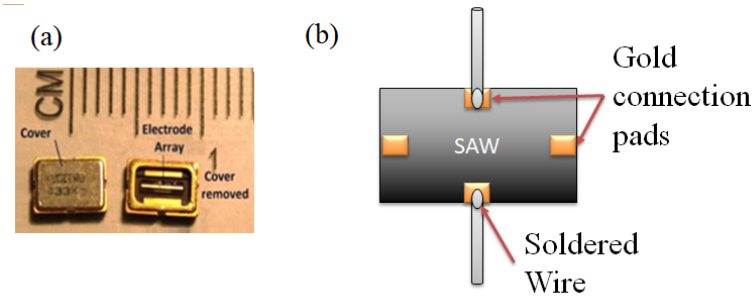

Figure 3.6: (a) Commercially available electrode chips, i.e. surface acoustic wave (SAW) resonator chips (Qualcomm B39431R880H210). The left one is opened for testing. (b) Two connection wires are soldered to pins on the back SAW chip in order to connect the electrodes to the measurement device.

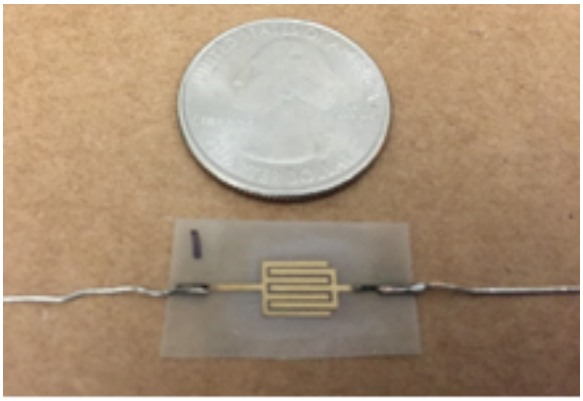

Figure 3.7: Copper PCB electrodes by chemical etching.

After being slipped into water to release the paper from image picture, the board is cleaned and dried, toner reactive foils is applied to seal the toner image against the etchant, resulting in a perfectly etched image. With the ink sealed and protected by toner reactive foils, the patented copper sheet is then immersed into copper etchant, or ferric chloride (MG Chemicals), which is heated to 55C (135F). After etching the board, toner reactive foils and underlying toner are removed by wiping down the board with Acetone.

3.3.2 Electrodes Surface Functionalization

Detection procedures are described as follows. Cleaned electrodes are functionalized with thiol modified probe for twenty-two hours in a humidor under room temperature. Surface Functionalization includes probe incubation and uncovered surface blocking The 1.0 mM 6-mercaptohexanol in ultrapure water is used as blocking reagent. The quality of electrode functionalization is monitored by measuring the Cint. After the DNA samples are diluted from stock samples, they are added onto the electrodes connected to an impedance analyzer for tests.

Before immobilizing the probe on the surface, the electrodes should be rigorously cleaned. The effectiveness of the cleaning procedure has been confirmed by significant decrease of the interfacial capacitance at the solution/electrode boundary[74]. The first part of the cleaning process consists of immersing the electrode into 100 nM sodium hydroxide (NaOH) and connect it to a potentiostat. As shown in figure 3.8 The electrode potential is swept from 0.3V to 1.1V . After 5 scans of cyclic voltammetry, the electrodes are rinsed with water.

Then, the chips are soaked in NaOH in a glass beaker on a hot plate-stirrer for 15 min then in acetone for 10 min. Later, they are rinsed by isopropyl alcohol for 10 s and deionized water for another 10 s, and dried by an air gun. To make it hydrophilic, the electrode surface are treated by a UV ozone cleaner for 15 min. Then the electrode surface is ready to be functionalized.

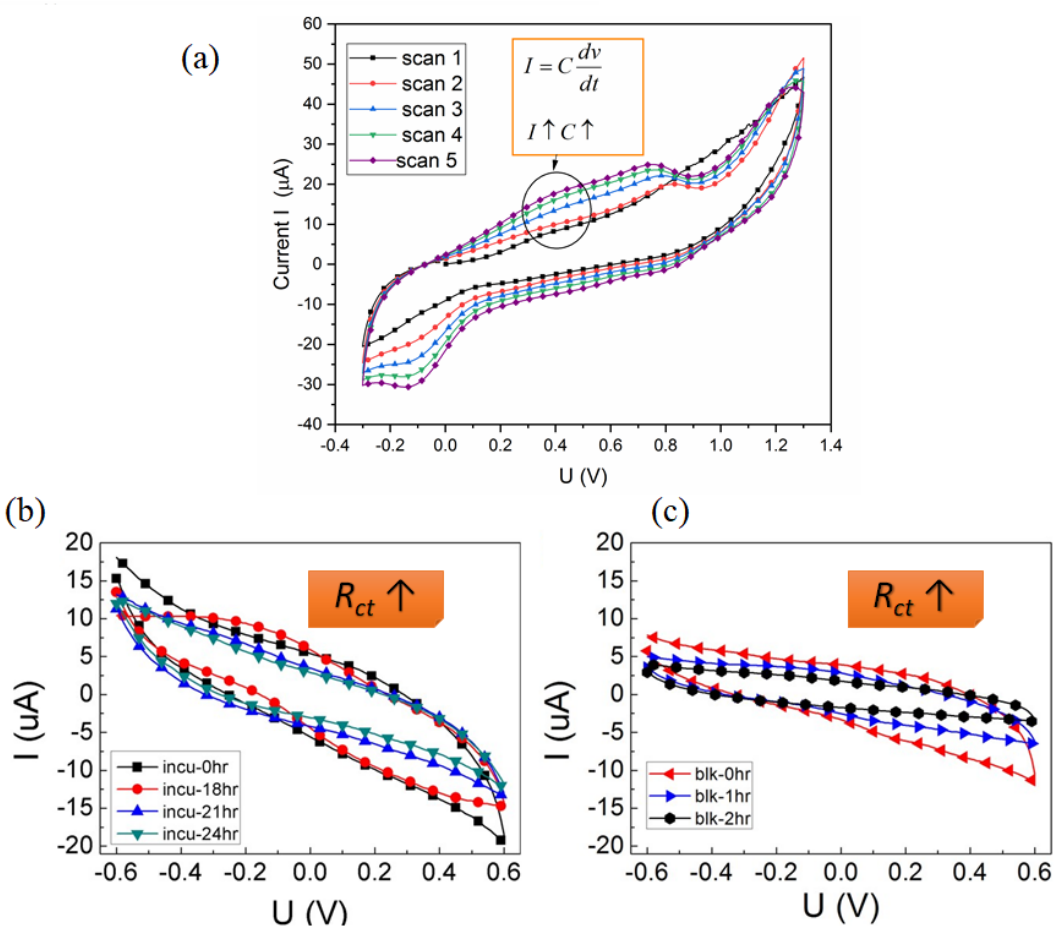

Figure 3.8: Cyclic voltammetry characteristics of sensors (a) cleaning, (b) incubation and (c) blocking process.

Chapter 4

Development of assay protocols for highly sensitive and specific on-site detection of Drugs and bacterial DNA

4.1 Detection of cocaine in human serum

Cocaine is one of the most used illegal recreational drugs. Developing an on-site test for cocaine has been a focus of research effort, since it is essential to the control and legal action against drug abuse. Currently most of cocaine detection methods are time-consuming and require special or expensive equipment, and the detection often suffers from high cross-reactivity with cocaine metabolites and relative low sensitivity with the best limit of detection reported at sub nanomolar (nM) level. In this work, an aptasensor has been developed using capacitive monitoring of sensor surface incorporating alternating current electrokinetics effects to speed up molecular transport and minimize matrix effects. The aptasensor is rapid, low cost, highly sensitive and specific as well as simple-to-use for the detection of cocaine from serum. The assay has a sample-to-result time of 30 s, a limit of detection of 7.8 fM, and a linear response for cocaine ranging from 14.5fM to 14.5pM in standard buffer, which are great improvements from other reported cocaine sensors. Special buffer is used for serum cocaine detection, and a limit of detection of 13.4 fM is experimentally demonstrated for cocaine

spiked in human serum (equivalent to 1.34pM cocaine in neat serum). The specificity of the biosensor is also demonstrated with structurally similar chemicals, ecgonine ethyl ester and methylecgonidine. This biosensor shows high promise in detection of low levels of cocaine from complex matrices.

4.1.1 AC electroosmosis for accelerated aptamer-Cocaine binding

In this work, ACEO microflows are expected to be more effective than DEP for cocaine enrichment due to cocaine's small size[16, 66].A non-uniform AC electric field induces counter-ions, which will move under the electric fields tangential to the IDE surface, generating swirls-like ACEO flows above the IDEs. Those flows carry the target (cocaine) towards the IDE surface, which speeds up the transport of target molecules to the electrode surface and bind with the immobilized probe. The relation between ACEO fluid velocity and the applied electric field is given by the following equation,

$$\upsilon_{ACEO} = \frac{-\epsilon_m}{\eta} * \Delta\xi * E_t \tag{4.1}$$

where ϵ_m and η are the permittivity and viscosity of the medium, E_t is the component of the electric field strength tangential to the electrode surface, and $\Delta\xi$ is the voltage drop over the interfacial layer including the EDL and molecular deposition at the electrode surface[66]. As discussed above, ACEO effect can induce microfluidic vortices above electrodes to accelerate the transport of cocaine molecules to the electrode's surface for binding[26], which significantly improves the detection sensitivity and response time. To promote ACEO effect, the test samples are diluted in electrolytes with low to medium ionic strength. As a result, the interface at the sensor/solution will exhibit a strong capacitive property with a high electric impedance. Therefore, a significant portion of the applied voltage will drop across the interface to produce ACEO flows[75]. Further, meso-size IDE arrays are adopted here based on the findings that large IDEs favor the generation of ACEK microflows to DEP effect[64]. To maximize the enrichment effect by ACEO, we further optimized the AC frequency of sensing signal.

4.1.2 Sample preparation

Chemical reagents are purchased from ThermoFisher (Grand Island, NY). Cocaine, ecgonine ethyl ester and methylecgonidine solutions are purchased from Sigma Aldrich (St. Louis, MO). The sample solution used for ACEK capacitive assay is based on 1: 100 dilution of 1xPBS (150 mM Na+) in ultrapure water (denoted as 0.01 x PBS). The sequence of 5 thiol modified cocaine specific aptamer is 5-ATCTCGGGAGACAAGGAAAATCCTTCAATGAA GTGGGTCTCCC-3 [35]. After aptamer immobilization, 1.0mM 6-mercaptohexanol in ultrapure water is used to block the electrodes. Cocaine hydrochloride solution (1.0 mg/mL in methanol) is diluted in 0.01xPBS to make stock solution. 0.01xPBS is used to serially dilute cocaine stock solution and make cocaine samples of 1pM, 100 fM, and 10 fM in 0.01xPBS, so that the ionic strength of samples are kept constant during all the serial dilutions. To test cocaine levels in human, human serum is 1:100 diluted in pure water. Then, cocaine is spiked into the aforementioned sample solutions. The sample collection is reviewed and approved by the institutional review boards of The University of Tennessee, Knoxville.

4.1.3 Surface functionalization

The detection of cocaine is performed using gold electrodes fabricated based on printed circuit board (PCB) technique with a simple and low cost process. After the cleaning, sensor functionalization includes immobilization of cocaine-specific probe and blocking the surface of the electrodes. The immobilization of the probe is performed by loading 10 μL of 10 μM cocaine-specific aptamer diluted in 0.01xPBS over the electrode and incubating it in a humidor for 24 h. 1.0 mM 6-mercaptohexanol is used to block the surface. After 3 h of blocking, the chips are ready for testing. Two types of control tests are carried out as well. One is testing the blank buffer solution (0.01xPBS) without target molecules by a functionalized sensor, and the other one is testing cocaine on dummy electrodes (electrodes that are blocked without probe immobilization), so as to gauge the magnitude of response artifacts caused by the applied electrical field.

4.1.4 Measurement and data processing

This work uses ACEO based capacitive sensing to monitor the probe/ target binding. The interfacial capacitance is found by measuring the electrode's impedance at a fixed AC frequency and voltage continuously during the testing. Using a high precision impedance analyzer (Agilent© 4294 A), the capacitance of the sensor is recorded through its LAN port and sampled 201 times for a duration of 30 s. Then, the percentage change of the measured capacitance per minute is found. The normalized capacitance change rate (d$|C|$/dt, where $|C|$ means normalized capacitance) is calculated for each cocaine concentration by applying the least square linear fitting. Each concentration is tested five times with a new functionalized sensor each time.

4.1.5 Results and discussion

Based on our prior work on ACEK capacitive sensing of small molecules[64, 76], an AC signal is applied at a specific frequency (1 kHz) and amplitude (400 mV) directly to the sensor for 30 s to induce ACEO effect and measure the capacitance change in real time. The choice of the signal amplitude is not arbitrarily. In fact, high voltage amplitude strengthens the ACEO flow and can enhance the cocaine binding. However, higher voltages may damage the surface functionalization of the electrode by causing the immobilized molecules to detach, leading to sensor malfunction. Based our previous calculation chapter 3, 1 kHz is chosen as our testing frequency.

Dose response and limit of detection (LOD):

To obtain the sensor's specific response to various concentrations of cocaine, 14.5 fM to 1.45pM of cocaine in 0.01xPBS is tested using functionalized and dummy sensors respectively. The dummy sensors do not have specific aptamers immobilized on them. Their responses will reflect how much artifact is caused by the applied electrical field. Each cocaine sample is loaded into a chamber sealed over the electrode surface. As shown in Figure 4.1, the normalized capacitance change rate increases with higher cocaine concentration. The d$|C|$/dt value is -3.77%/min for 14.5 fM cocaine and reaches 7.16%/min, and -10.44%/min for

145 fM and 1.45pM of cocaine, respectively. The capacitance change rate for the blank control solution without cocaine is -0.97%/min, which is negligible in comparison to those triggered by cocaine in the samples. It is also important to notice that the responses for 14.5 fM to 1.45pM of cocaine by the dummy sensors are no more than 1.92%/min. These results confirm that the changes of $Cint$ mainly come from the binding of cocaine molecules with the aptamer. Based on Figure 4.1, the sensitivity of the sensor is calculated to be $\frac{dC}{dt}(\%/min) = -1.446ln(x) - 0.0725$, where x is cocaine concentration in fM. The sensor response is linear over the tested range from 14.5 fM to 1.45pM. The cut-off response of the sensor is defined as 3 standard deviations from the response of background solution. Consequently, the cut-off value for sensor response (d|C|/dt) is found to be -1.22%/min . By substituting this value into the dose response equation, the LOD is calculated to be 7.8 fM cocaine.

Selectivity:

For a biosensor to be practical, selectivity is one of the critical attributes that is highly desired for biosensors[61]. Here, the specificity of cocaine sensor is tested against methylecgonidine and ecgonine ethyl ester, two chemicals that are structurally similar to cocaine. With cocaine-specific aptamer, the capacitance change rates for 10pM of methylecgonidine and ecgonine ethyl ester are -1.18 $\pm$ 0.13 %/min and $-1.22 \pm 0.16\%/min$, respectively, as shown in Figure 4.1 . Obviously, the sensor's responses for both chemicals at 10pM are more positive than the cut-off value for the sensor, thus considered as non-responsive.

Serum samples:

The performance of this biosensor in a real life setting is evaluated by detecting cocaine in biological complex samples. Human blood serum is chosen for this test. First, the effect of serum matrix is studied by testing 14.5 fM, 145 fM and 1.45pM cocaine spiked in 1:100 diluted serum. The sensor responses for the background solution and interference molecules are found to be considerably larger for the spiked serum samples than those in 0.01xPBS.

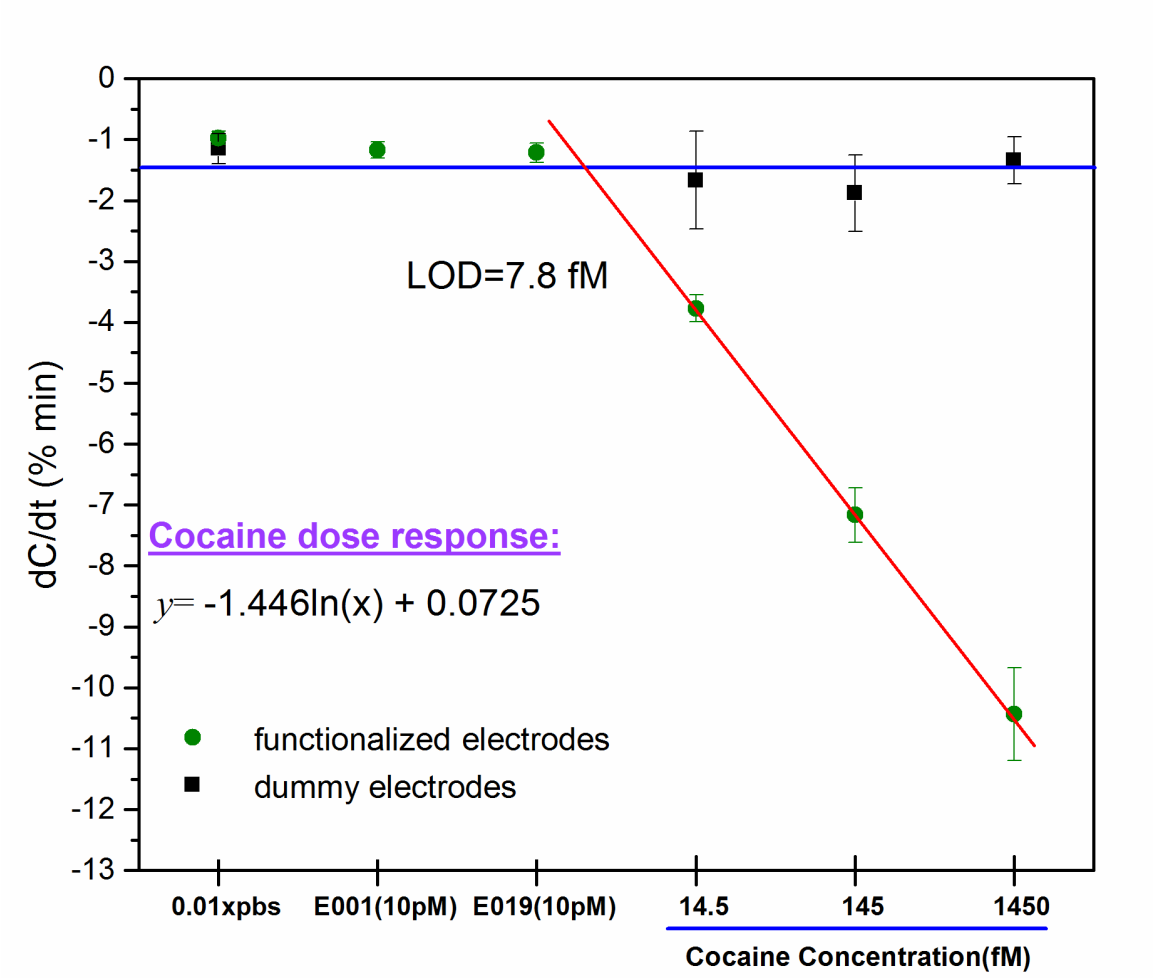

Figure 4.1: Response of cocaine in 0.01xPBS on both functionalized sensors and dummy sensors. The response of the functionalized sensors to the background (0.01xPBS) and the two structurally similar chemicals are also shown here, and their magnitudes are less than the cut-off value. Each data point is the average of five repeated tests. Error bar indicates standard deviation. The red slanted line is the extracted dose response.

As shown in figure 4.2, the sensor responses are $-2.04 \pm 0.16\%/min$ and $-2.36 \pm 0.68\%/min$ for diluted serum (the background) and 10pM methylecgonidine (the negative control). The capacitance change rate of 14.5 fM cocaine spiked in serum became $-2.93 \pm 0.92\%/min$, and is no longer distinguishable from that of the background or the negative control values. Again, the d$|C|$/dt of the cut-off response is found by subtracting 3 standard deviations ($30.16\%/min$) from the response of the background solution (-2.036%/min). This value is then substituted in the dose response equation, y1 = -1.318ln(x) + 0.2518 and the LOD is calculated to be 126 fM. This degradation in sensitivity can be explained by the deposition of interference molecules (proteins) in serum on the surface of the sensor. We improved the testing buffer by adding proteinase into serum.Proteinase K can break down proteins in the serum[77]. 10 mg/mL of Proteinase k is diluted 1:20 in 0.01xPBS. The neat serum is then 1:100 diluted in the aforementioned solution. After loading 10 μL of serum samples spiked with 14.5 fM to 1.45pM cocaine, the d$|C|$/dt magnitude is observed to gradually increase with increasing cocaine concentration. The three cocaine serum samples and the background are clearly differentiated from each other. The responses are $-3.92 \pm 0.46\%/min$, $-7.95 \pm 0.82\%/min$, and $-11.08 \pm 0.40\%/min$ for a cocaine concentration of 14.5 fM, 145 fM and 1.45pM, respectively. The dose response is linear from 14.5 fM to 1.45pM, and can be expressed as y2 = -1.557ln(x) + 0.0939. For the background and 10pM methylecgonidine, the $|C|$ values are $-1.23 \pm 0.15\%/min$ and $-2.16 \pm 0.04\%/min$, which are smaller in magnitude than those in diluted serum without protease. The LOD is calculated to be 13.39 fM, equivalent to 1.34 pM in neat serum. A comparison of the responses between two types of buffers shows that adding proteinase K to the testing buffer has significantly improved the sensitivity of the sensor, and also decreases the responses from serum background.

To sum up, without any signal amplification or use of label, the detection of cocaine molecules can be accomplished within 30 s. The developed sensor shows a linear detection range from 14.5 fM to 1.45pM of cocaine with a limit of detection of 7.8 fM in PBS or 1.34pM in neat serum. The use of Proteinase K helps to break down the proteins in the serum, and as a result, no purification is needed for testing serum samples.

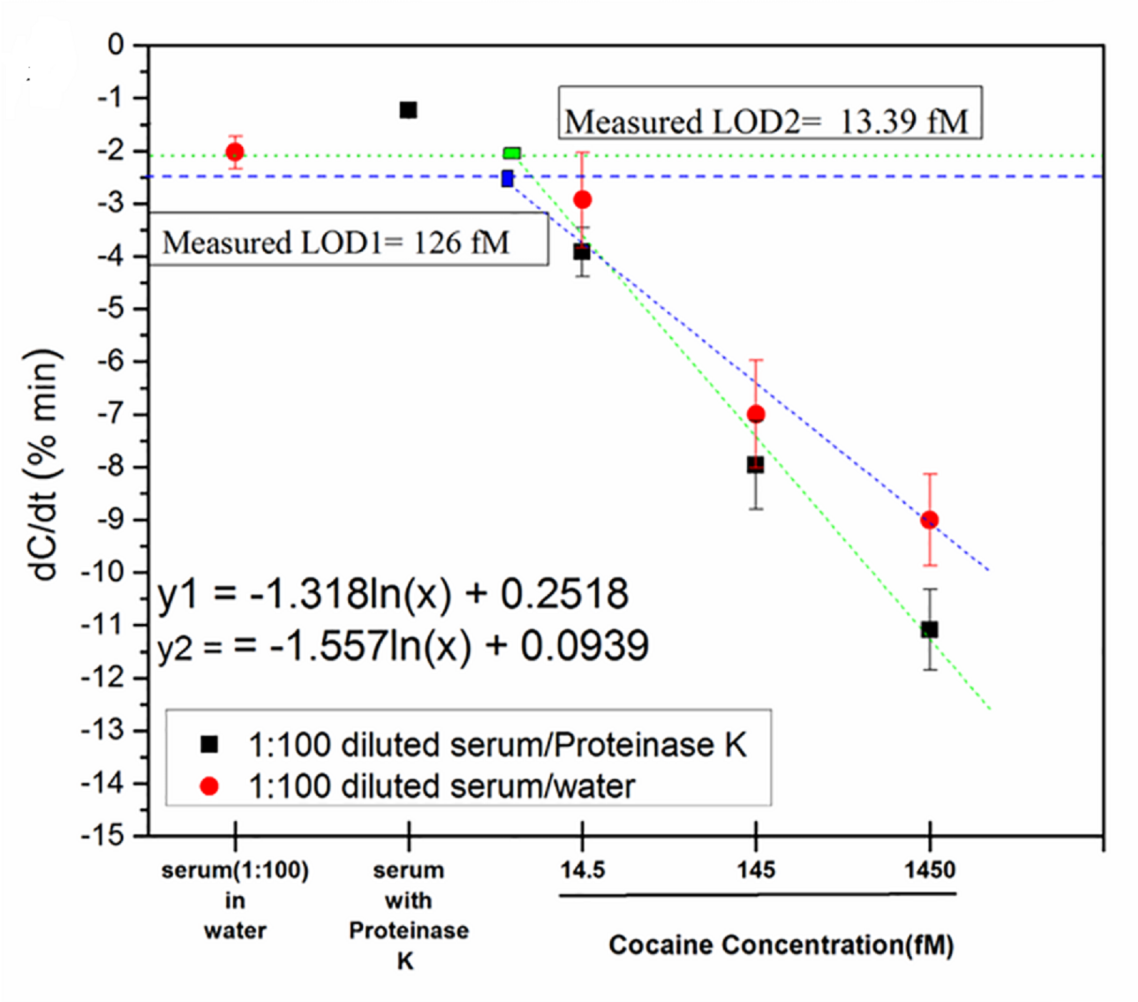

Figure 4.2: Sensor response to different concentrations of cocaine samples. The dotted line is the extracted standard curve. The sensor sensitivity is the slope of the extracted curve. The horizontal lines indicate the cut-off d$|C|$/dt values of the sensor response, which correspond to 126 fM when serum samples are diluted only in pure water and 13.39 fM cocaine when proteinase K is added to the testing buffer. Error bars represent standard deviation.

4.2 Detection of MRSA Genomic DNA

Antimicrobial resistance is quickly becoming a public health issue of increasing significance. Methicillin resistant Staphylococcus aureus (MRSA) is one of the most common causes of hospital and community-acquired blood stream infections. Timely treatment with appropriate antibiotic therapy is essential to combating the infections and its further complications. There is growing urgency for rapid, sensitive, specific and simple-to-use identification methods for MRSA. Conventional culture methods are time and labor consuming while molecular diagnostic tests require well trained personnel and expensive laboratory equipment. This work reports a genomic DNA (gDNA) sensor using a probe targeting mecA gene for on-site screening of MRSA within 10s. Innovation includes low voltage dielectrophoresis (DEP) enrichment of gDNA molecules for rapid hybridization and high sensitivity; and simple, direct measurement of interfacial capacitance with minimal matrix effects. Through engineering a balance between the DEP attraction and DNA charge repulsion, differentiation between MRSA and similar gDNAs such as those of methicillin susceptible S. aureus can be achieved. The outcome is a label free, sensitive (with a detection limit of 3.2 copies/L MRSA gDNA) and specific DNA capacitive sensor with potential for point of care diagnosis.

4.2.1 Materials

PBS (0.05x) used for probe incubation in this work is prepared by 1:20 volume dilution of commercial physiological strength 1x PBS (containing 75 mM of sodium chloride, pH 7.4, Thermo Fisher Scientic, Waltham, MA, USA) in ultrapure water (Mili-Q). Blocking solution used for blocking the uncovered sites on functionalized electrodes is 1.0 mM 6-mercaptohexanol (Sigma-Aldrich,St.Louis,MO,USA) prepared in ultrapure water. Testing buffer is based on saline-sodium citrate (20x SSC) buffer. It is purchased from AccuGENETM (Lonza, Rockland, ME, USA) and then diluted to make 0.5x SSC in ultrapure water. Two 5thiol modied MRSA probes are used. Probe EB (5-TTACAGAGTTAACTGTTACC-3) is designed to specically target femB gene which codes for an enzyme in various different Staphylococcus spp including methicillin resistant

Staphylococcus aureus (MRSA) and methicillin sensitive Staphylococcus aureus (MSSA). Probe MEC (5-GTAGAAATGACT-GAACGTCCGATAA-3) is designed to specically target mecA gene which is only found in MRSA but not MSSA[78].

Genomic DNAs of MRSA(ATCC 700699D-5) and MSSA (ATCC 25923DQ) are prepared in ultrapure water at concentration of 2.7 and 1 ng/mL, respectively, as stock sample solution.

4.2.2 Assay protocol

The detection of MRSA DNA is performed using both saw chips and gold IDME. 10 μL of working uid are loaded on the electrode's surface. Detection procedures described as follows: cleaned electrodes are functionalized with thiol modified probe for twenty-two hours in a humidor under room temperature. For MRSA testing, the double strands of MRSA DNA should be separated (denatured) to allow the hybridization on the aptamer incubated on the IDME electrode. To get a single strand DNA (ssDNA), thermal denaturation is operated [79]. After the DNA samples are diluted from stock samples, they are heated on a dry bath at 95C for 10 min, then chilled onto ice for 1 min. At a room temperature, they are added onto the electrodes connected to an impedance analyzer (Agilent 4294A) for tests. A high precision impedance analyzer (Agilent 4294A) is used to apply the symmetric AC signal continuously for 10 seconds across the sensor. The interfacial capacitance of the sensor C_{int} is recorded through its LAN port. Then, the percentage change of the measured capacitance per minute is calculated. The normalized capacitance change rate (d$|C|$/dt%/min where $|C|$ means normalized capacitance) is used to indicate specific hybridization level of MRSA DNA.

4.2.3 Sensor performance under different voltages

Ideally, specific binding should lead to a decrease in Cint due to close contact between the probe and target, while non-specific binding should cause no change or little increase in $C-int$ due to the loose interaction between nonspecific DNAs to electrodes. This phenomenon has been verified by our past work (see figure 4.3) [80, 81].

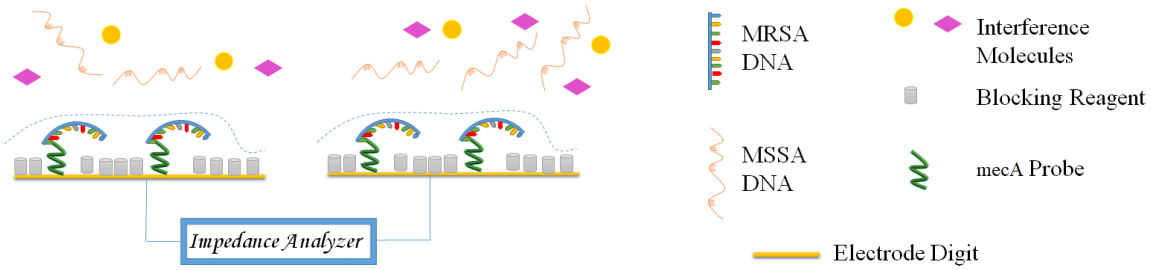

Figure 4.3: Schematic of MRSA DNA capacitive sensing. On the electrodes surface (yellow bars), MRSA molecules are attracted toward the electrodes surface by DEP force. After decreasing the probe density, hybridized probe-gDNA duplex can lie closely to the electrodes and lead to a decrease in Cint for specific detection.

Hence, the measuring AC signal and buffer conductivity are carefully chosen to make pDEP effect strong to attract DNA molecules and decrease Cint and yet not so strong for the detection to be non-specific. MRSA samples (positive samples) and E.Coli (non-specific binding) in 0.5xSSC are tested with three different voltages (7, 10 and 15 mV).

The sensor responses are plotted in Figure 4.4. Three voltages of 7 mVrms, 10mVrms and 15 mVrms are tested under the same conditions of frequency and sweep time as mentioned above. The change rates that indicate the adsorption level of MRSA DNA are significantly higher than those from the control and interference samples except for the results at 7 mVrms. The sensor response to 2.7ng/ml MRSA DNA (2501.4 copies/μL) is $-1.45 \pm 0.51\%/min$ at 7 mVrms, which is signicantly lower than those at 10 mVrms($-3.05 \pm 0.36\%/min$) and 15 mVrms ($-3.16 \pm 0.36\%/min$), demonstrating that 7 mVrms is insufficient to induce any ACEK effects and AC electrical eld indeed assists hybridization at a voltage equal or higher to 10 mVrms. As sensor specicity is essential to biosensor operation, the sensor response to E.coli (non-target samples) can be clearly distinguished from those of MRSA DNA samples when 10 mVrms is applied to the sensor.

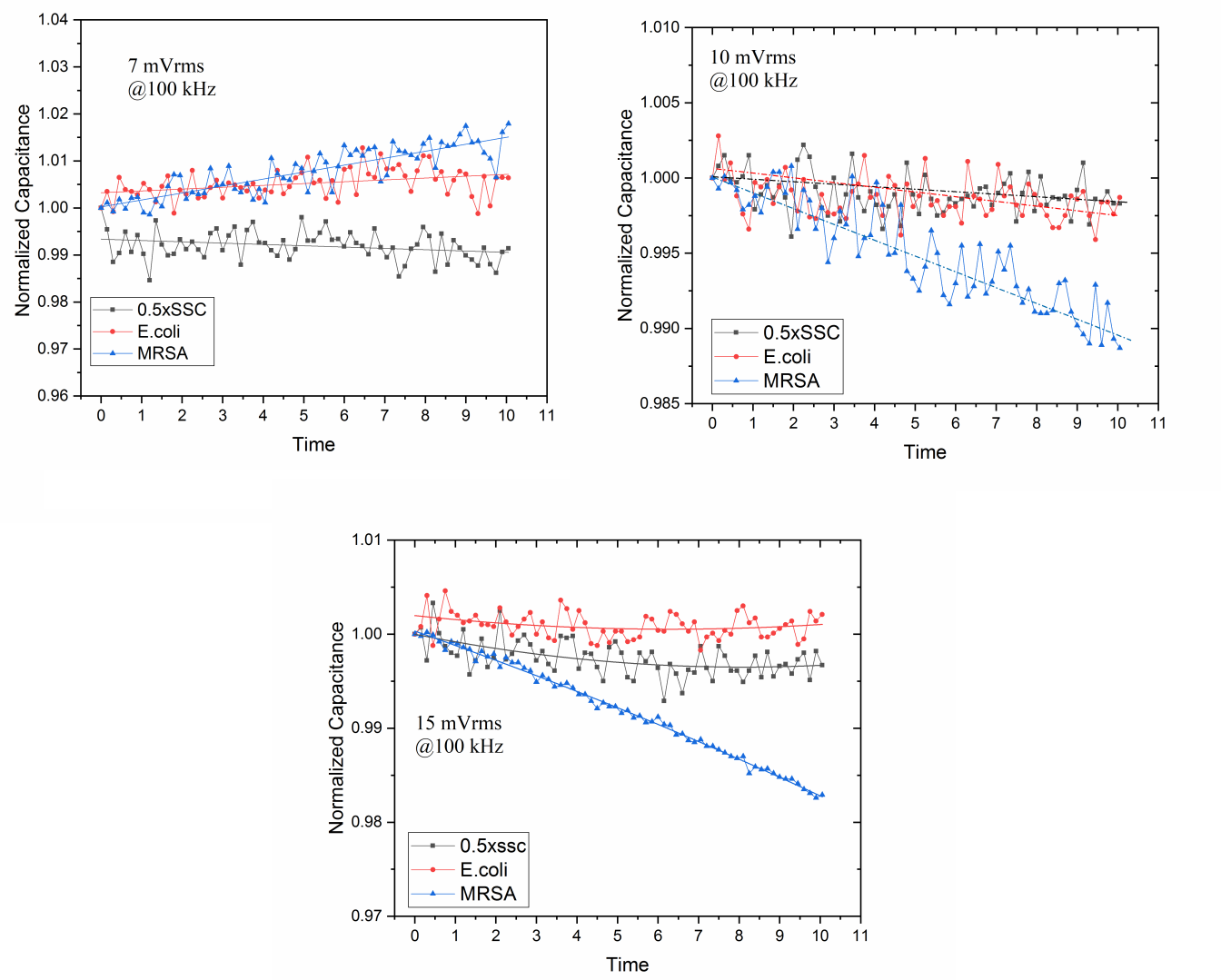

Figure 4.4: Voltage optimization for MRSA Detection: Three different voltages 7 mVrms, 10 mVrms, and 15 mVrms are tested. 10 mVrms is adopted for subsequent experiments..

In fact, at 15 mVrms, DEP force becomes stronger and attracts other interference molecules randomly , including E.coli samples. Hence, 10 mVrms is adopted in our protocol.

4.2.4 Optimization of assay time

Next, the assay time is optimized for this MRSA detection method. Our previous work on protein and small molecule detection found that capacitance change rate taken over different time period correlates with the analyte transport process[81, 82]. Because DEP attraction decays with distance, gDNAs travel towards the sensor is slower for those farther away from the electrodes, so the hybridization events become less frequent with time. In this test (figure 4.5), the same AC signal is applied to the sensor with three different sweep times (10, 20 and 30 s).

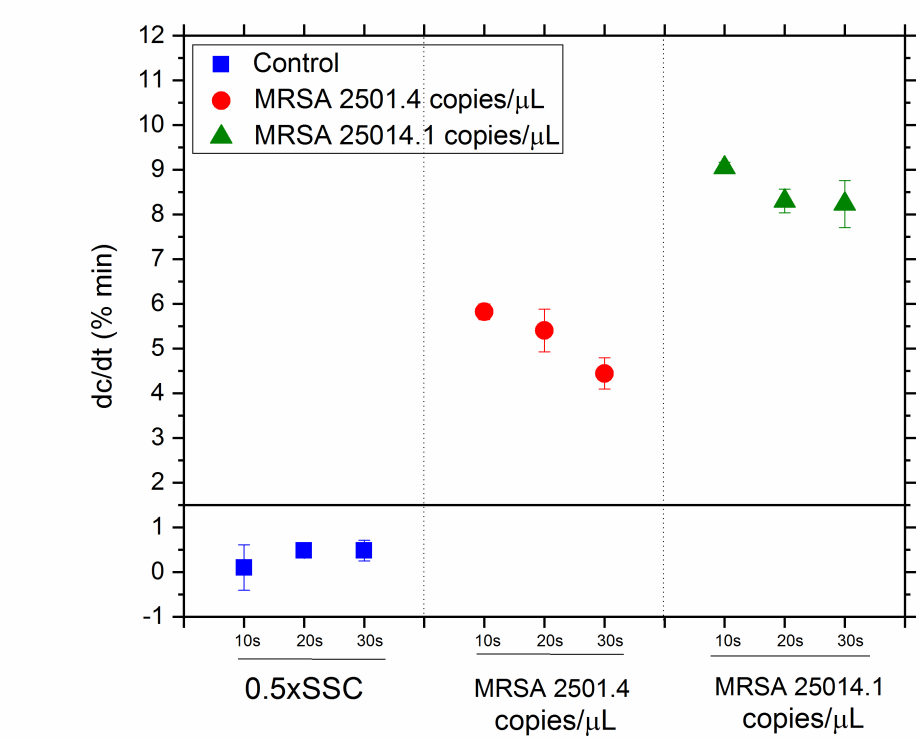

Figure 4.5: Evaluation of sensors response of two MRSA samples concentrations (2501 and 25014 copies/ L) under three different assay times (10, 20 and 30s). 10s is the optimized assay time as its gives the highest response.

Two MRSA concentrations (2501.4 and 25014.4 copies/μL) in 0.5xSSC are measured for this optimization process. Using 30s, 2501.4 and 25014.4 copies /μL of MRSA gDNA have the responses of 4.44±0.35% and 8.23±0.53% per minute. When the sweep time decreases from 20 s to 10 s, the response of the sensor to 2501.4 copies/μL MRSA gDNA increases from 5.40± 0.47%/*min* for 20 s to 5.82±0.18%/*min* for 10 s. Similarly, the sensor response of 25,014.4 copies/μL MRSA gDNA increases from 8.30±0.26%/*min* for 20 s to 9.04±0.13%/*min* for 10 s. The change in capacitance becomes slower with time, thus indicating a transport process by DEP. There is a very little responses change for from the control sample, attesting to the specificity of this gDNA sensor. The assay time is set to be 10 s from this point on.

4.2.5 Selectivity by probe density optimization

The probe density on a sensor also plays an important part to sensor performance. In biosensor development, it is typically desired to have as high probe density as possible to obtain large sensor response. Based on our prior work, initially, the sensor surface is incubated with 10 μL of 2 μM mecA probe solution[61]. As shown in Figure 4.6,

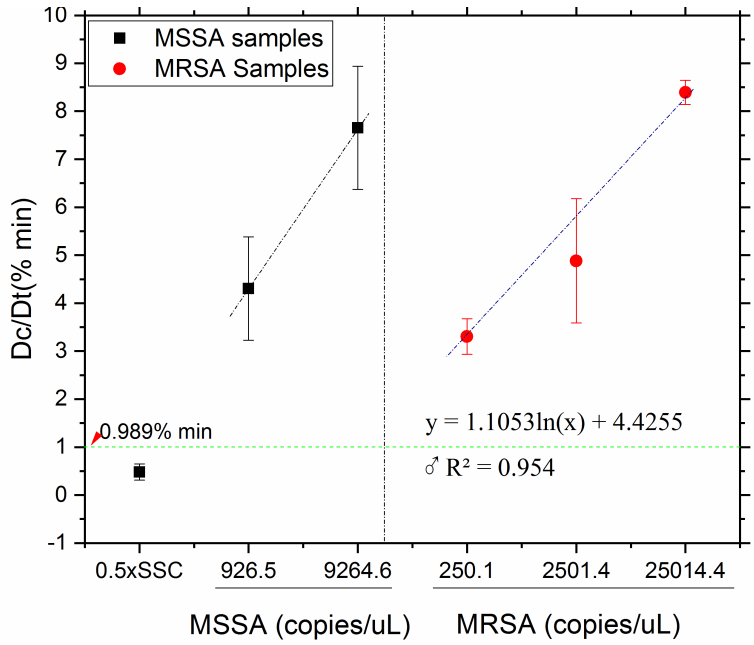

Figure 4.6: Response of MRSA and MSSA samples in 0.05xPBS tested on Au-PCB electrodes incubated with 2 μM of mecA probe. The capacitive response is similar between specific and non-specific binding.

270 pg/mL (250.1 copies/μL), 2.7 ng/mL (2,501.4 copies/μL) and 27 ng/mL (25,014.4 copies/μL) are the tested concentrations of MRSA samples spiked in 0.5xSSC. Each sample is tested in quadruplicate and their results are 3.30±0.37%/min, 4.88±1.29 %/min and 8.39±0.25%/min respectively, with the response of the buffer solution 0.5xSSC at 0.48±0.16 %/min(background). As sensor specicity is essential to biosensor operation, two concentrations of MSSA samples at concentrations of 926.5 and 9,264.5 copies/μL are also tested to determine the sensor specificity to Methicillin-resistant S. aureus.

While the sensor yields high response to MRSA samples, capacitive responses can not be distinguished between positive and negative samples, and Cint is increasing for both specific and non-specific samples. Ideally, specific binding should lead to a decrease in Cint due to close contact between the probe and target, while non-specific binding should cause no change or little increase in Cint due to the loose interaction between nonspecific DNAs to electrodes. This phenomenon has been verified by our past work [80, 81]. We therefore, hypothesize that the higher coverage of the surface leads to high charge density at the electrode surface, which in turn leads to repulsion between the electrode surface and genome sequence. While the DEP force is able to attract the gDNA to the sensor surface for hybridization, the rest of gDNA sequence is away from the surface and suspending in the solution. The gDNA electrically connects with the sensor surface, expanding the surface area of interfacial capacitance, resulting in an increase in Cint (see figure 4.7), which cannot be separated from non-specific binding at low concentration of gDNA.

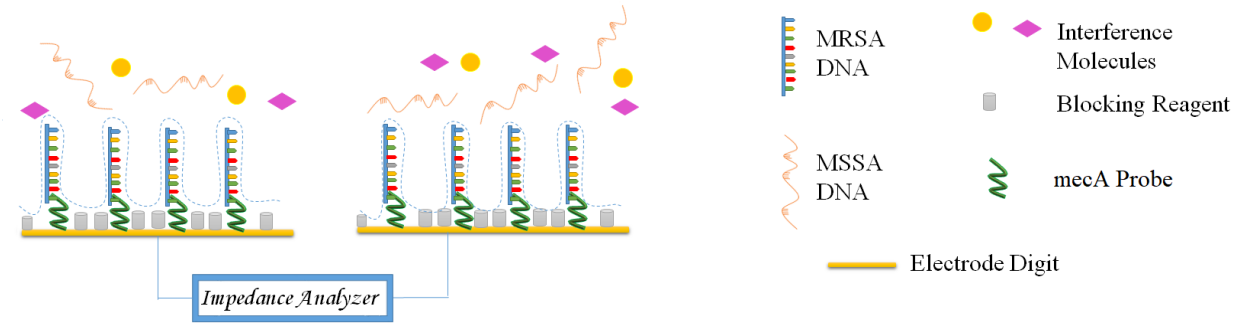

Figure 4.7: Schematic of MRSA DNA capacitive sensing. On the electrodes surface (yellow bars), MRSA molecules are attracted toward the electrodes surface by DEP force. The high surface coverage of mecA probe creates more negative charges which repulse the target DNA and the duplex probe-target is loosely packet. Hence, C_{int} increases.

Hence, we have decided to reduce the probe density 2M to 200 nM so that hybridized probe-gDNA duplex can lie closely to the electrodes and lead to a decrease in C_{int} for specific detection (as in figure 4.8) . Indeed, with the reduction of probe density, the capacitance change for MRSA gDNA reverses its direction, and now MRSA and MSSA can be clearly differentiated.

4.2.6 Higher sensitivity by changing electrode design

In the previous experiment, lower probe density improves the selectivity of the sensor but it also decreases the sensitivity of the sensor. The LOD is also worse since 2501 copies/μL cannot be distinguished from the background. A lower LOD is desirable for better clinical

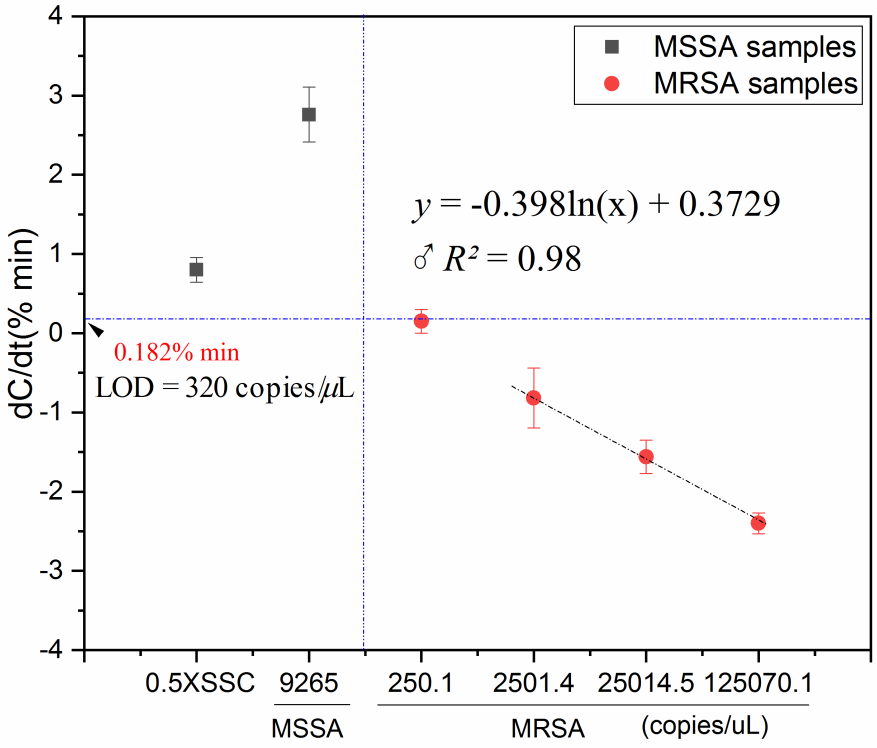

Figure 4.8: Response of MRSA and MSSA samples tested on Au-PCB electrodes incubated with 200 nM of mecA probe in 0.05xPBS. The capacitive response reversed the direction and is decreasing for the specific binding and increasing for nonspecific binding. LOD is defined as 3 standard deviations from the average response of the background control (0.5xSSC).

performance of the sensor. According to equation 3.3 (see Chapter 3), DEP is more pronounced with smaller electrodes. Hence, in the next step, electrodes with small critical dimensions are used to enhance the sensitivity of our capacitive assay. They are Surface Acoustic Wave (SAW) electrode chips and modified from Qualcomm B39431R880H210. Each electrode finger is 2.0 μm wide, 170μm long, with 1.5 μm spacing from each other. Around 10μL of sample can be accommodated by the metal housing around the electrode chip. As demonstrated in Figure 4.9, the capacitance change rates are higher with SAW electrodes (around 4 times higher than Au-PCB responses) with $d|C|/\mathrm{dt}$ values for 0.27, 2.7 and 27 ng/mL of MRSA are -3.37 $\pm$ 0.30%/min, -4.5 $\pm$ 0.52%/min and -6.72 $\pm$ 0.87%/min, respectively. The modified sensor shows a logarithmic dependence on MRSA

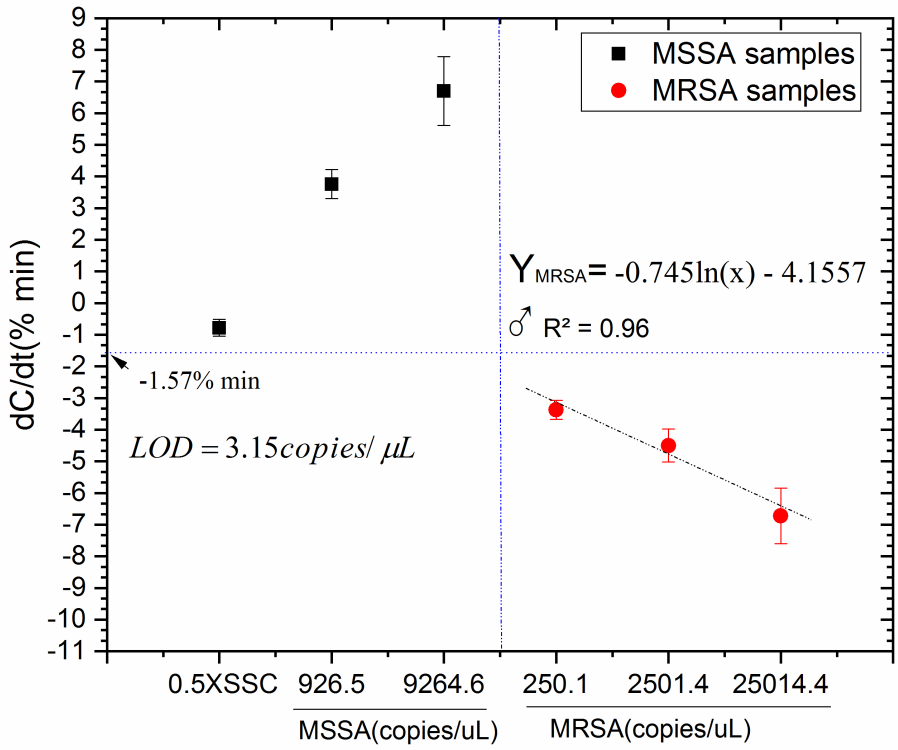

Figure 4.9: Response of MRSA and MSSA samples tested on SAW electrodes incubated with 2 uM of mecA probe. The capacitive response is decreasing for the specific binding and slightly increasing for MSSA binding in 0.5xSSC

concentration ranging from 0.27 to 27 ng/mL and the dose response is calculated to be $y = -0.745ln(x) - 4.1557$ where x is concentration of MRSA in 0.5xSSC.

Based on the definition, the cut-off value for sensor response ($d|C|$ /dt) is found to be -1.57%/min. By substituting this value into the dose response equation, the LOD is calculated to be 3.4 aM (3.15 copies/μL) in 0.5xSSC.

4.2.7 Testing mixture

Due to close similarity between the gDNAs of MRSA and MSSA, the sensors specificity is tested in two sets of experiments. In the first set, the sensor is incubated with probe EB (5-TTACAGAGTTAACTGTTACC-3) designed to detect femB gene, which is a common gene in both MRSA and methicillin susceptible S. aureus (MSSA) [83, 78]. We first tested different concentrations of MRSA and MSSA seperately on SAW chips incubated with 2 μM of EB probe.

The results are summarized in Figure 4.10. Each sample is tested four times on a new functionalized sensor each time. The sensor, as shown in Figure 7a, responds similarly to MRSA and MSSA when targeting the common gene (femB). The sensitivity of the sensor is calculated to be ($d|C|$/dt) = -0.788ln(x) -2.2651 where x is S. Aureus concentration and the LOD is calculated to be 135 copies/μL in 0.5xSSC.

To sum up, By testing for hybridization signal with capacitive afnity sensor based on ACEK, it is possible to confirm detection of MRSA DNA using a specific probe sequence for the mecA gene. Without any signal amplification or use of label, MRSA DNA detection can be accomplished within 10 s response time with a LOD of 3 copies/μL in 0.5xSSC.

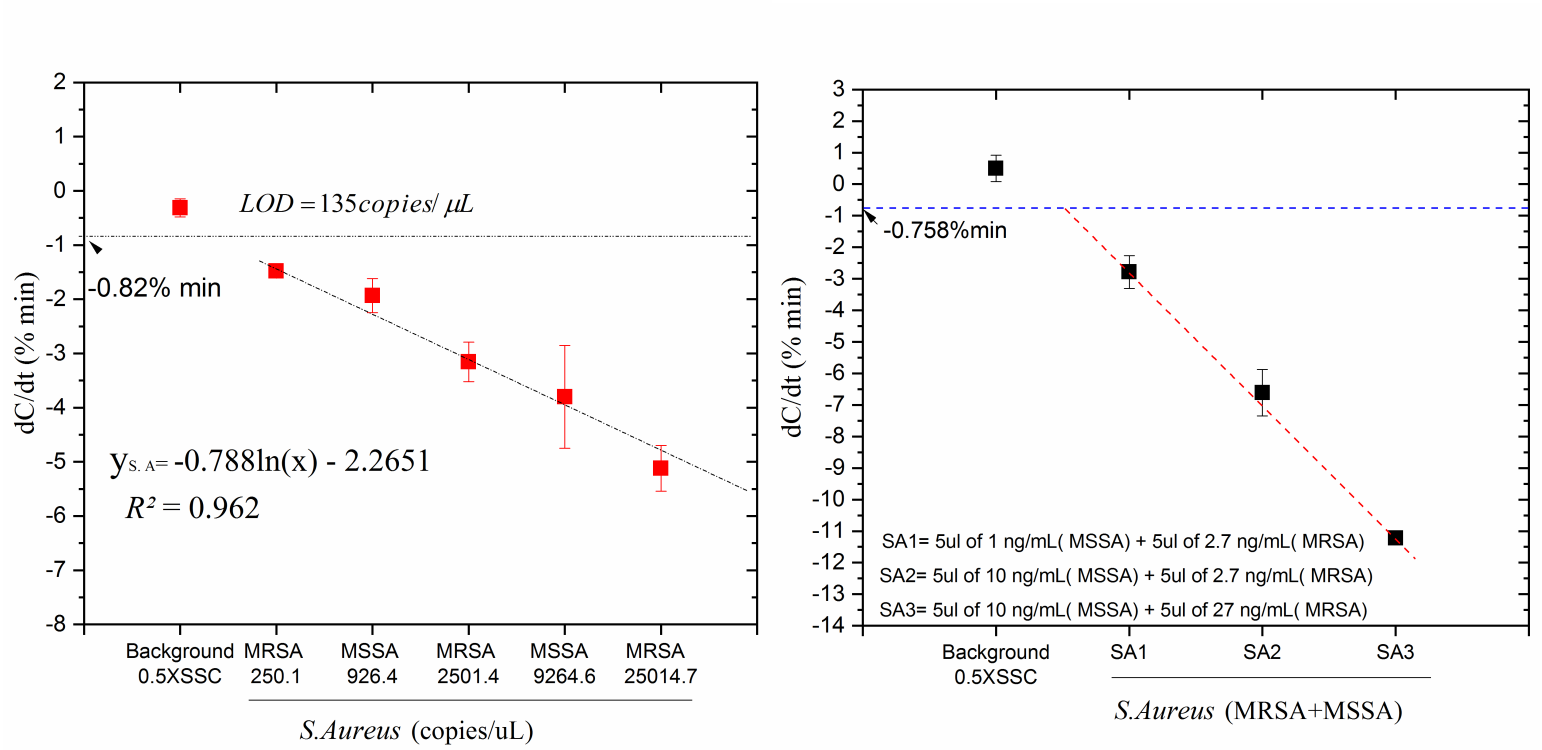

Figure 4.10: (a) Dose response from SA Detection on SAW electrodes incubated with 2 μM EB probe. (b)Sensor Specificity: dose response from MRSA in the presence of other analog gDNA strains (MSSA) with similar and higher concentrations.

Chapter 5

ABC readout system Design

The foregoing chapters describe the characteristics of AC signals when detecting two main categories of targets (drugs and pathogens). This chapter describes how to design a portable capacitance reader to meet the requirements of detecting drugs and pathogen DNAs by ABC sensing.

Based on the previously mentioned detection requirements (specific AC voltage, frequency), the details of the design of the portable readout system are provided in this chapter. This chapter explains the architecture of the ABC platform and its components functionality. This includes the circuit design of the system modules to calculate the electrode impedance. It also explains the analog design of the proposed system.

5.1 Work motivation

The concept of ACEK capacitive sensing is validated by, Agilent 4294A (Agilent, USA), to detect cocaine from serum samples and bacterial DNA, a benchtop precision impedance analyzer, is used to perform one channel ACEK capacitive sensing. Currently, there is an unmet need in the market for a capacitance analyzer that meets the requirements of the multiplexed ABC sensing. Its primary requirements are (1) to not only operate in analytical laboratories but also to be embedded and portable , i.e. being light weight, small and user friendly; (2) to provide custom and adjustable excitation signals for ABC sensing, e. g. 75 kHz at 10mVrms with zero DC bias;(3) Multiplexing sensing for panel detection is also

highly desired. The motivation of the work is to construct a simple impedance meter based on the AD5933 IC for measuring impedance sensors used in microbiology. This work presents early design of a three sensors impedance measurement circuit dedicated to bio-impedance embedded applications. It extends the use of the AD5933 measurement chip to allow it to operate in low voltage configuration (10 mVrms) for viral and bacterial DNA detection and high voltage configuration (300 mVrms) for Drugs and large molecule detection.

5.2 Design consideration

The capacitance change studies over a range of frequency is used to determine that 1k to 100k Hz input sinusoidal wave has to be applied to the sensor to get a impedance change that is directly related to the concentration of respectively cocaine and MRSA samples . Moreover, the designed platform should be able to generate a wide range of amplitude sinusoids (from 300 mVrms to as low as 10mV RMS) with a zero DC bias to be suitable for viral and bacterial DNA detection. This implies that the readout system should be able to generate signals of different amplitude and frequency.

While detecting cocaine samples in human serum, the difference in capacitance change between 100fM and 1pM is the smallest capacitance difference for a ten time sample concentration increase. We calculate the lowest impedance change between the two cocaine concentrations to be 2nF which is the one between (151 nF, 149 nF). This requires that for accurate detection, the readout system must be able to correctly detect an impedance change as low as 1nF (half of the 2nF).

To design the final smart biosensing platform, the work is split into two major sets of experiments:

- High voltage(up to 2vpp) multiplexed sensing platform:

The focus here is to design an embedded capacitance acquisition platform that is suitable for ABC sensing, i.e.from 1kHz up to 100 kHz and zero-DC biased AC signal with high amplitude to induce ACEK effects, such as 2Vp-p. In this 3 channels multiplexed sensing board, 2 channels are dedicated to simultaneous measurement of the electrodes capacitance.

The third channel is for system calibration. The excitation AC signal from the embedded impedance analyzer is customized to be suitable for bacteria and drug detection.

- Low voltage Multiplexed sensing platform:

This system adopts the multiplexed sensing design to measure the electrode capacitance accurately. Also, to be suitable for viral and bacterial DNA detection, we extend the use of the AD5933 measurement chip to allow it to operate in low voltage configuration (10 mV). Different frequencies will be selected for each sample.

5.3 System development and experimental design of the multiplexed sensing platform

5.3.1 Readout system overview

Figure 5.1 shows the photo of the portable ABC bio-diagnostic platform. The schematic and the layout of the designed board are given in the next subsection.

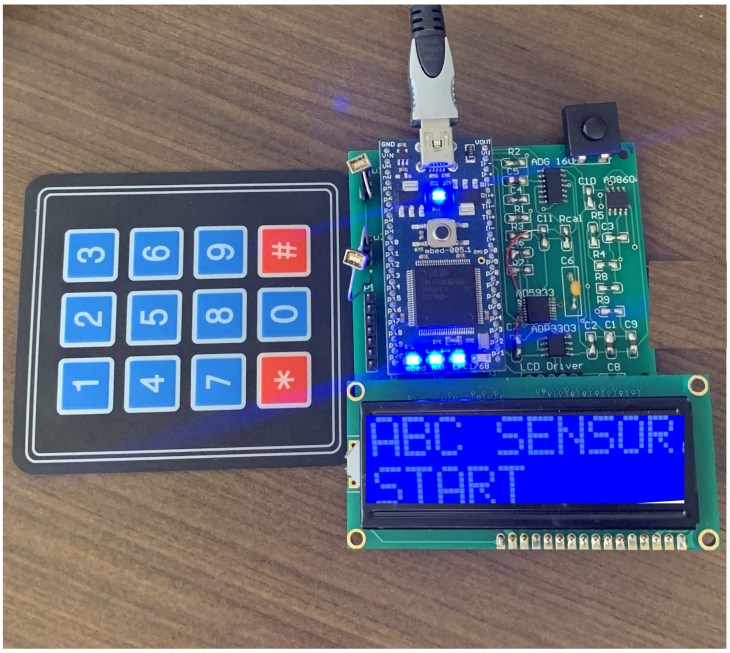

Figure 5.1: Photo of the portable ABC bio-diagnostic platform

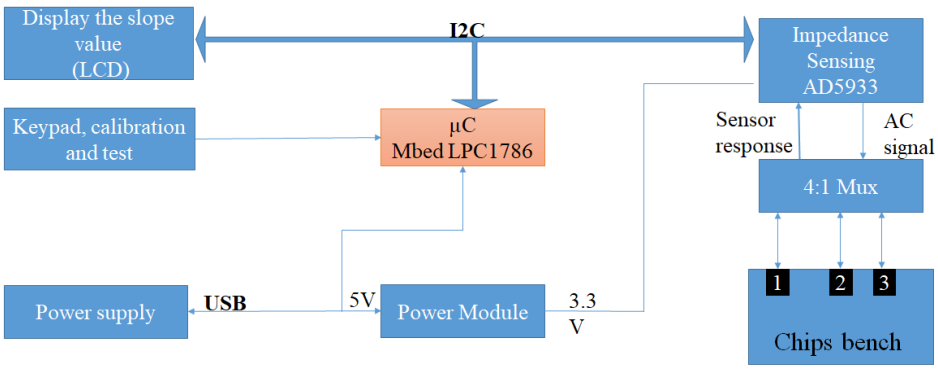

Figure 5.2: Block diagram of the design of the designed ABC sensing system.

The designed board is mainly include a microcontroller unit (MCU) of mbed LPC1768 development board (ARM, England), an IC for impedance measurement AD5933 (Analog Devices, USA), a 4:1 Mux (ADG1604) and other ICs as opamps. Two peripherals are used to communicate with the user: a 4by4 keypad (Adafruit, USA) and an LCD screen (Adafruit, USA) with its driver soldered on the backside. The board is powered by a micro-USB cable which is also used for data transmission. SAW chips and PCB electrodes are used here as our test sensors . The block diagram of the designed system is shown in 5.2

Using this multiplexed sensing platform, target detection is designed to be an easy and single-button operation. The electrode is inserted into the board and a 10μL of diluted clinical sample is loaded onto the chip surface. As shown in the following flowchart, the ABC device is powered up with a USB cable to start measurement. The microcontroller idle for 0.1s to reach the steady state of the ICs. To guide the user, messages is displayed on the LCD screen as "Initialization..please wait ", "Press any button ". Meanwhile, MCU will initialize the remaining components and set the excitation AC signal specifications (voltage frequency) output from the impedance analyzer IC. After the initialization, a function of sensor ′ calibration is carried out automatically to calculate the "gain factor" and hence accurately calculate the capacitance values from the test measurement. More details are provided in the next section. The operator then choose which frequency to use to test the samples(options of selecting different frequency for different samples) and trigger the detection process. During 30 sec detection, the sensor is excited by the AC signal, the

response signal of each electrode is sampled for 200 points at an interval of 150 ms, the Mux switches from a channel to another at a rate of 220 ns.

The microcontroller will read the real and the imaginary part of the sampled impedance value through serial inter-integrated circuit (I2C) interface to calculate the capacitance and its change rate. The operator will read on the screen the results within 30 sec and file will be stored in the MCU memeory to provide detailed information of the calculation (impedance, time, phase and rate). Finally, the system will idle until the next detection is initialized.

To design the schematic of the ABC readout system, a modular approach is adopted. As shown in figure 5.3, The board is divided into three major modules:Power, Multiplexed sensing,and Computing module (MCU). MCU is responsible for controlling the workflow and data processing; the sensing module reads the sensors capacitance and sends data to the MCU, and the power module regulates the required voltage and power. Further details of the three modules are discussed in the following sections .

5.3.2 Multiplexed sensing module

- AD5933 - commercial impedance analyzer chip

This is the most important component in the multiplexed sensing module as it measures external complex impedance by exciting it with a generated sinusoidal signal from pin Vout (pin 6 of AD5933). The frequency of the sinusoid can vary from 1 to 100 kHz, and its amplitude voltage from 200 mVpp to 2 Vpp (with DC offset) depending on the user settings through the I2C. Then, the current flowing through the unknown impedance is measured , sampled into 1024 samples by the on-board ADC and DFT processed to return a real (R) and imaginary (I) data-word for complex impedance calculation. The AD5933 generates the output sine wave signal using the DDS algorithm. Either an internal clock (16MHz) or an external clock system can be used as the reference clock to the IC. The same selected clock will be assigned to the 12 bits ADC inside the AD5933.

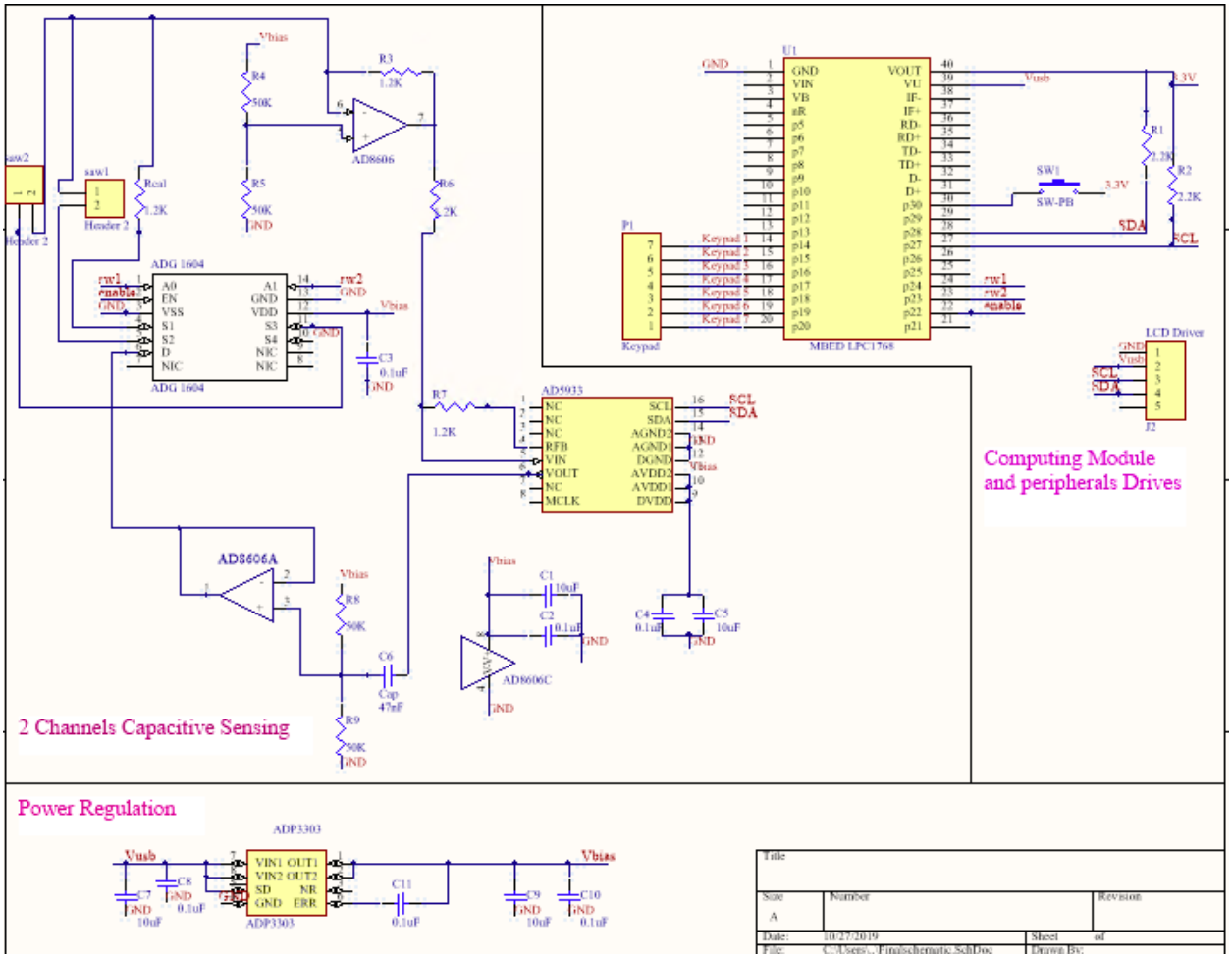

Figure 5.3: Schematic design of the developed ACEK capacitive sensing system.

As our ACEK assay protocols require a frequency range from 3 to 100 KHz, the internal clock frequency will be used to generate the signal. Also, in order to do the frequency sweep and extract the impedance value at each point, the sweep frequency range and its increment factor should be programmed by specifying the start frequency, frequency increment and number of increments register in the register map[4]. By configuring the start frequency to 10 kHz and step size to zero, a single frequency measurement is achieved. Another parameter that should be considered while configuring this IC, is the number of settling cycles which indicates the waiting time before the ADC starts sampling the output in terms of number of output cycles[4]. This allows to start testing right after the system reaches a steady state.A C++ function is programmed to verify whether a single point frequency sweep is completed or indicate the entire frequency sweep is done. Once the sweep is complete, the real and imaginary values are stored in two different registers and a repeat frequency sweep command is sent to the control register.

Although the AD5933 is a very powerful and efficient chip, it suffers from some drawbacks that currently prevent its use for bio-impedance measurements, specifically on a microscopic scale. First, while the AD5933 has four programmable output voltage ranges of 1.99, 0.97, 0.383 and 0.198 Vp-p. To each aforementioned voltage level, a DC bias exists (respectively 1.48, 0.76, 0.31, and 0.173 V).Moreover, the internal current to voltage (I-V) converter inside the AD5933 is VDD/ 2 biased. Thus, at the pin Vin, the received voltage is an AC ground with a DC level set at 1.65 for a VDD=3.3 V. This circuit design imposes the presence of a DC potential difference between Vout and Vin pins of AD5933. The presence of this DC bias, at the interface between the electrodes and the samples solution, may alter the medium to be measured and cause reading errors[84]. Also, It can lead to unsought consequences due to electrochemical reaction.

- Analog signal conditioning chain

As aforementioned, independently from the value of the selected output voltage level, there is a potential difference between Vout and Vin pins of the AD5933 no matter what output voltage is selected. So, an extra analog circuitry should be implemented to to condition the output signal from pin Vout of AD5933, crossing the electrode and returning back

the Vin pin of AD5933.This extended circuit will initially remove this DC component to avoid impedance misreading. Applying 4 equal DC levels at the other side of the electrode will counter the existing 4 DC levels across the tested sensor. But, this direct solution demands the implementation of extra DC voltage conditioning circuits and exact control of DC voltage levels in the circuit.Hence,this solution is abandoned.The implemented solution is to reconstruct the DC bias configuration as shown in figure 5.4.

Initially, we thought of biasing the output signal at ground. However, as this chip works on a single supply then, the output signal would be clipped off On the negative side. Hence,both ends of the electrode should be biased at the same DC potential. This last is fixed at VDD/2 (1.65V) as the VIN pin shown in figure 5.4 is internally biased at VDD/2. The output voltage from pin Vout is then filtered using a high-pass filter. 47 nF capacitor and a 50 k resistor are used to build the filter with a corner frequency at about 67.8 Hz. Using two resistors, the signal is biased again. Then, in its voltage follower configuration, One channel of the amplifier AD8606 (ADI, USA) is specified to buffer the signal.

The excitation signal is applied to one side of the electrode. Another AD8606 connected to the second terminal of the electrode is added in an inverting amplifier configuration to

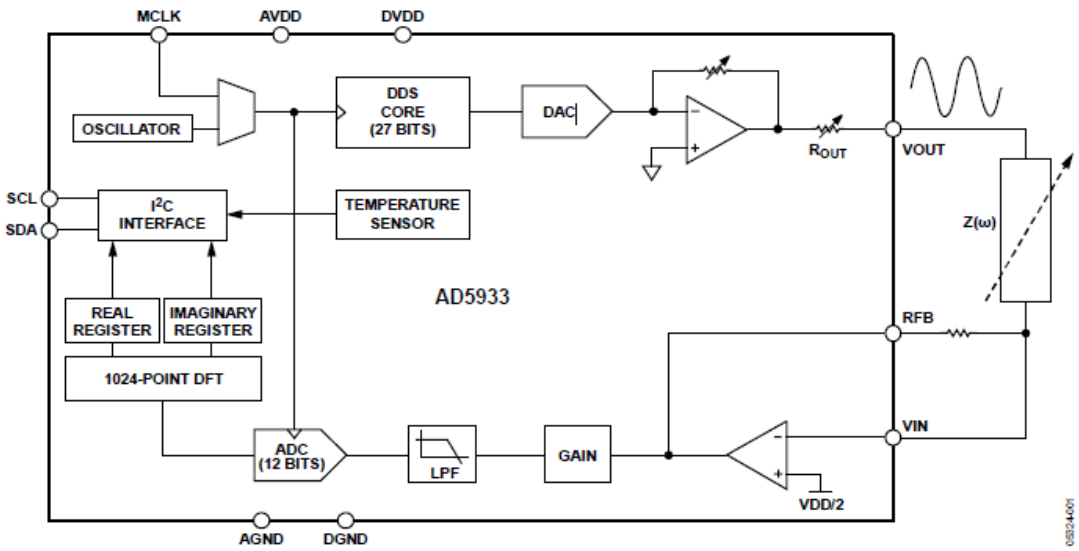

Figure 5.4: Functional block diagram of AD5933 (from Data sheet) [4]

remove 180-degree phase shift of the applied signal. To ensure that the difference in DC bias across the sensor is removed, this op-amp must be also biased at VDD/2. Before feeding this signal to the input pin of AD5933 (vin), the internal amplifier of the impedance analyzer chip is configured to unity.So, two identical resistors are connected to Vin and pin RFB of AD5933.

System calibration step begins when the conditioned excitation signal outputting from the buffer reaches the CMOS analog multiplexer. ADG1604 is a 4 channel Mux that operates bidirectional. This chips operates as a switch between the calibration channel and the sensing channel. This allows to calibrate and measure different sensors impedance without the user intervention. In addition, it gives the option to sense up to 3 different impedance simultaneously.

Wide range of commercial multiplexers, covering single to multiple switch elements with various signal ranges, are available in a variety of packages to meet customer application needs. However, deciding on optimal multiplexer for this work can be a tricky task. In this project, ADG1604 is a complementary metal-oxide semiconductor (CMOS) analog multiplexer offered by Analog devices, it switches one of four analog input signals to a common output, D, as determined by the 3-bit binary address lines, A0, A1, and EN. Logic 0 on the EN pin disables the device. The following performance specifications are considered in the selection of the mux.

On resistance: Ron is the resistance of the closed switch path between the drain and source terminal. As we are measuring the impedance of biosensors, RON is in series. Therefore, the lower the on resistance, the better the system resolution and the less distortion. ADG1604 has Ron=1Ω . This ultra-low on resistance value makes this mux ideal for our application (as data acquisition and gain switching application). The on-resistance profile is very flat over the full analog input range, ensuring excellent linearity and low distortion when switching between sensors.

Capacitance and charge injection: In this work, we adopt capacitive sensing to detect the binding. Indeed, minimizing the capacitance of the switch is an important key specification to be considered. In fact, both the source and drain capacitances, when the switch is switching between on and off, are the cause of glitch impulse transferred from the digital input to the

analog output during switching, called charge injection. Thus, when the capacitance of the switch is low, generally the charge injection is also minimized. ADG1604 has a low digital input capacitance (CIN =8 pF) and the charge injection Qinj= 60 pC when VDD= 3.3V.

Switching rate: A switch is needed between the calibration channel and the sensors. In this design, ADG1604 is the chosen switch. The switching rate ton, as noted in the datasheet, is 227ns when VDD=3.3 V.

The value of calibration resistor is 1.2 kΩ as is the median value of our tested impedance values. The used electrode are measured previously by Agilent 4294A and their impedance ranged from 800 Ω to 1.6 kΩ. As the maximum voltage generated is 2 Vp-p, the maximum current flowing the impedance is 1.25 mA (found using R=800Ω)and then the input voltage of AD5933 will be $1.25mA * 1.6k\Omega = 2Vp - p$ which is less than 3.3V and then the internal amplifier of AD5933 is always operating in its linear region.

5.3.3 Computation module and peripherals

The microcontroller is the brain of this module. It is responsible for managing the overall workflow and communicating with the user through its peripherals.(As shown in the following flowchart 5.5) The MCU in this application is mbed LPC1768, which is an Advanced RISC Machine (ARM) ARM Cortex-M3 based microcontroller featuring a high level of integration, easy communication with the user and low power consumption. The serial clock line (SCL) and serial data line (SDA) for I2C are controlled respectively via pin 27 and 28 of the microcontroller and pulled up by two 2.2 kΩ resistors. The LCD with its driver and AD5933 are then connected to the I2C interface as I2C slave. The pin 22 and 23 and 24 are controlled as digital output to enable and command the MUX. A membrane keypad is connected to pin 14 →20. C++ is the program language in this design. Mbed online compiler is used to ccompile and built this application.

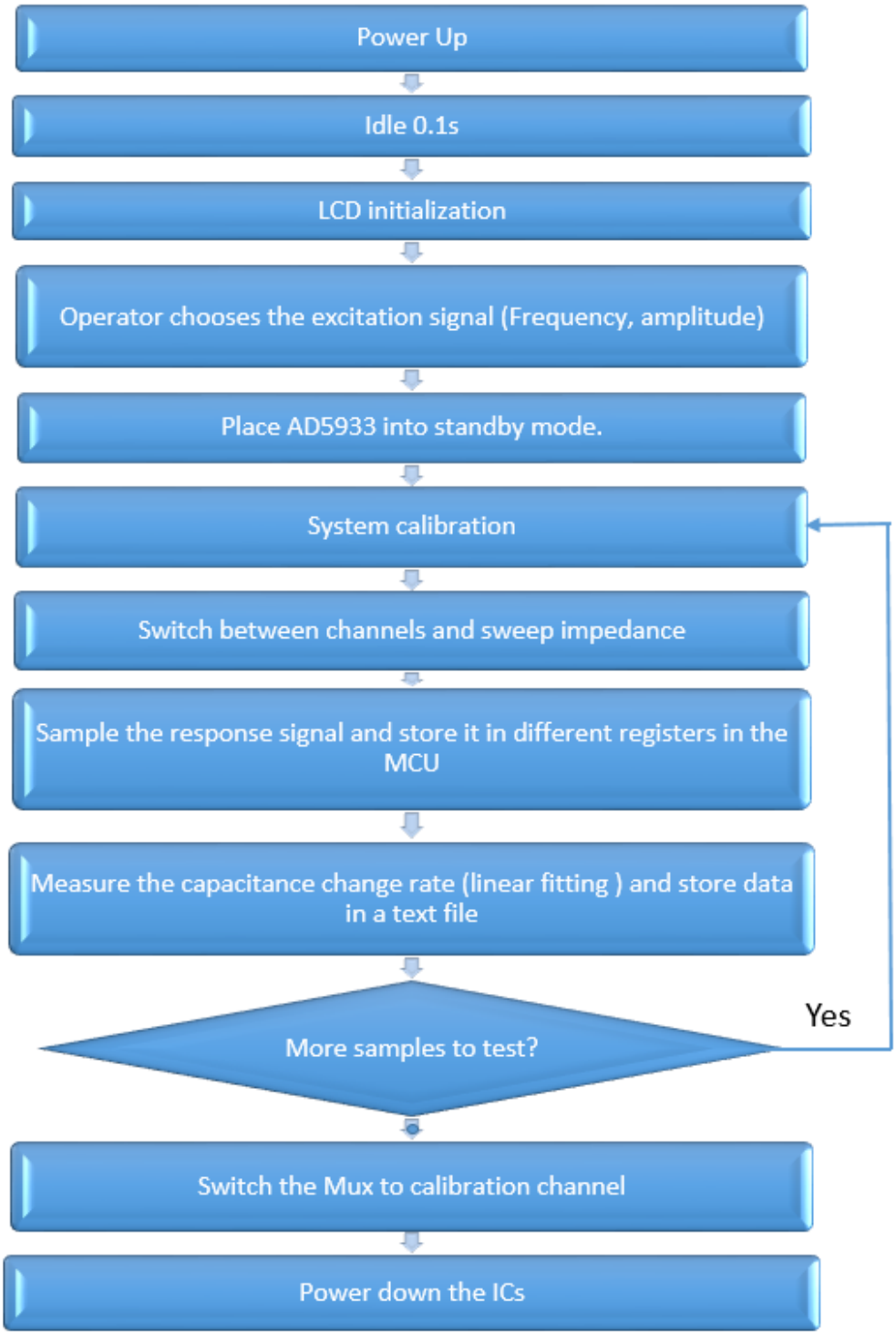

Figure 5.5: Workflow of the developed ABC sensing system.

The main function programmed in this module is to calibrate and calculate the sensors impedance. Since there will also be parasitic impedance signals from components other than the sensor in the signal path, the actual impedance measured by AD5933 needs to be calibrated to factor out the parasitic. This step is fundamental for an accurate measurement of sensor capacitance by our portable system. Hence an impedance with a known value (Z_{cali}=1.2kohm) is connected between the output and input terminals of the impedance analyzer. The measured value of its magnitude ($Magnitude_{cali}$) and system phase ($\phi_{measured,cali}$) are used for the measurement of the unknown sensor impedance in the next function (sweep impedance). A scaling factor called the gain factor ($Gain$) and an intrinsic system phase angle (ϕ_{system}) are then compared with the true values to prepare for the measurement of the actual unknown impedance. The gain factor ($Gain$) and the system phase ϕ_{system} are calculated respectively in equation 5.1 and 5.2 :

$$Gain = \frac{|Z_{cali}|}{Magnitude_{cali}} \tag{5.1}$$

$$\phi_{system} = \phi_{measured,cali} - \phi_{cali} \tag{5.2}$$

where $Magnitude$ is the square root of the results in the real data and imaginary data registers.

Once the calibration is computed, the unknown impedance can be measured by

$$Z_{sensor} = Gain * Magnitude_{measured,sensor} \tag{5.3}$$

and the sensor phase is measured by

$$\phi_{sensor} = \phi_{measured,sensor} - \phi_{system} \tag{5.4}$$

Then the imaginary part of the sensor impedance, its capacitance, can be found by:

$$Z_{Cap,sensor} = Z_{sensor} * sin(\phi_{sensor}) \tag{5.5}$$

The calibration impedance Zcali is selected to be a resistor for the sake of simplicity. A resistor with a resistance of Rcali has an impedance magnitude $|Z_{cali}| = \sqrt{Rcali^2} = Rcali$ and its phase angle ϕ_{cali}=0. To get more accurate results, the calibration impedance is tested 5 times and averaged to obtain the magnitude and phase angle. The calibration step should be done again as soon as the board powers up or a change in the excitation signal occurs.

5.3.4 Power Module

This ABC smart platform can work with a 4.5-9V battery. In our work, Pin 39 of the microcontroller provides a 5V transmitted through the USB cable. As our MCU has an onboard low dropout voltage regulator (LDO) LD1117S33 (ST Micro, Swiss) with a dropout voltage typically around 1 V. This voltage is used to pull-up the I2C only. However, most of the components require a 3.3 V voltage to turn on. For that purpose, ADP3303 which is a high accuracy linear regulator with a dropout voltage of 180mV at 200mA, is used to power the rest of the board components The input supply to this chip is selected from pin 39 (Vusb) of the MCU. To reduce noise, all the power source pins are coupled to ground using both 10 μF and 0.1 μF capacitors.

5.4 PCB design of the readout system

After selecting the right components, a schematic of the board is created using the software Altium Design. Most of the component ICs in our impedance measurement system are analog. (The mixed signal IC AD5933 is also considered as an analog IC). One ADP303 is used to provide one power plane for the rest of the circuit. We design our circuit to have only one ground trace. Later, a layout is exported from the designed circuit. The components are manually placed and routed.

The mesh of air wires are cleared up and organized to facilitate routing and so optimize final board area and layers. Then, each air wires is routed to a physical track with a width of 10mil. The required track width can be calculated based on the carried current and the thickness of the copper cladding to make the tracks. The completed layout of the board can be seen in 5.6. The manhattan style is adopted for the routing. The design rule check (DRC) and electrical rule check (ERC) are then completed to confirm the match between the schematic and layout and verify that the minimum spacing and size clearance are respected in the design. The 3D layout of the board is shown in the following figure5.7:

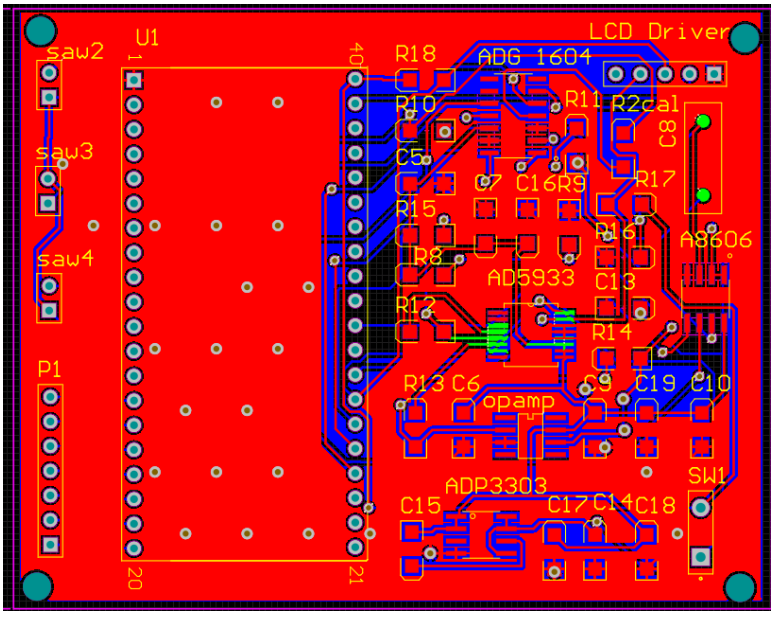

Figure 5.6: Completed layout of the readout system

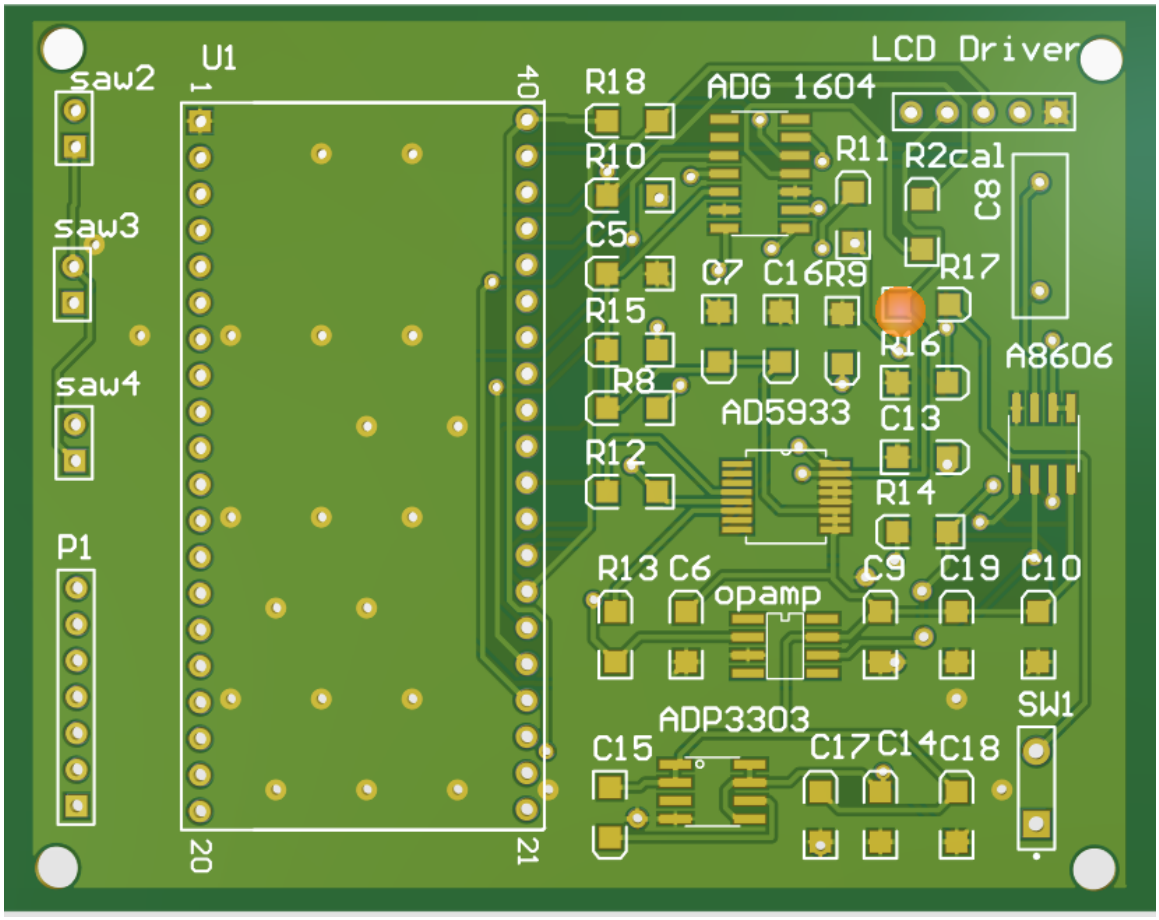

Figure 5.7: 3D layout of the ABC readout system

Chapter 6

Experiments and system testing

6.1 ABC system calibration test

As aforementioned in the previous chapter, calibration step plays an important role for the accuracy of the impedance measurement. In that sense, a sanity check are conducted to prove that the designed portable system is able to measure correctly a known value before testing an unknown value of the sensors impedance. A 1.2 k ohm resistor is used for calibration as it is the mean value of the tested sensors impedance (800Ω-1.6 kΩ). As shown in figure 6.1 the

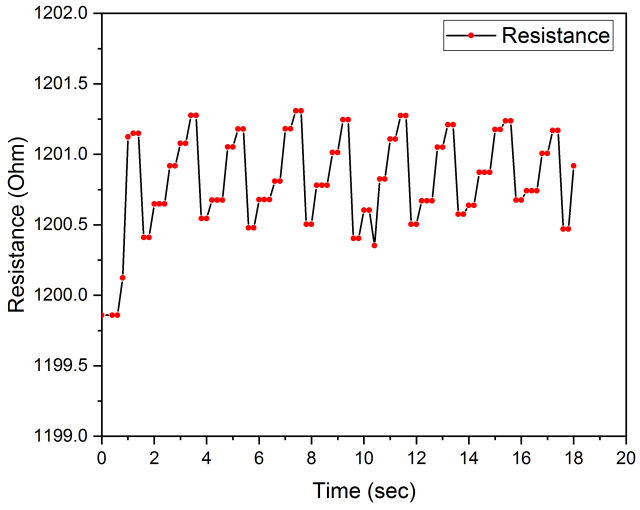

Figure 6.1: 50 times of measurements for a 1200 resistor. The mean value is 1200.267874 and the standard deviation is 0.09119

calibration resistor is measured 90 times in 18 sec for precision evaluation. The maximum and minimum measured values of the resistor is 1201.31Ω and 1199.85Ω respectively. The mean value of these 90 values is 1200.81582Ω and the standard deviation are 0.33585Ω. the figure 6.1 is an indication of the high accuracy of the device.

6.2 One channel impedance measurement

Before measuring multiple sensors simultaneously, the performance of the developed platform is first tested with one channel detection. Multiple tests are carried out to determine whether the device can detect impedance changes accurately and stably.

The tests consisted of respectively measuring simple resistance, complex impedance and saw chips impedance. Here, the measurement frequency of the system is fixed at 100 kHz with AD5933 output excitation voltage 2 Vpp (DC bias 0.76 V).

To verify that the external analog front end circuit enables us to apply a zero biased signal across the sensor, oscilloscope plots are recorded in figure 6.2.

Besides checking the voltage across the sensor, the performance of the analog circuit is tested by recording the input voltage of AD5933 and tracking its amplitude changing by

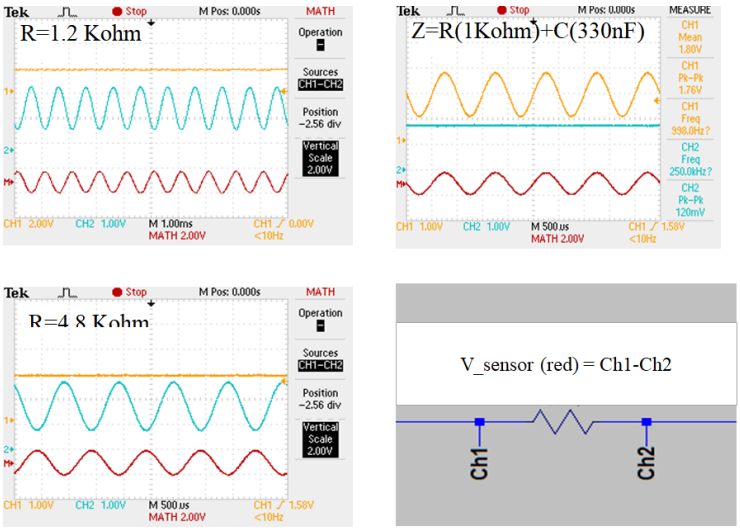

Figure 6.2: Oscilloscope plots showing the specification of the AC excitation signal across the sensor

testing different impedance. Two complex impedance (Z= $Z_R + Z_C$) are tested to mimic the electrode model(R in series with C. see3).

As shown in 6.3, when the impedance value is equal to the calibrated impedance, it is shown that the amplitude of the input signal is the same as the outputs signal which confirms that the system is well calibrated. However, by increasing the impedance magnitude, the input signal magnitude(correlated to the current owing through the tested impedance) decreases. To make sure that this portable reader is able to accurately measure the tested sensors, different impedance(resistive and complex impedance)are measured and its accuracy is determined. The figures 6.4 shows the comparison of the impedance results between the ABC sensor and a commercial multimeter the different impedance values percentage error for all the measured impedance.The complex impedance consists of R and C in series to mimic the equivalent circuit of the actual sensor. The value of the measured magnitude

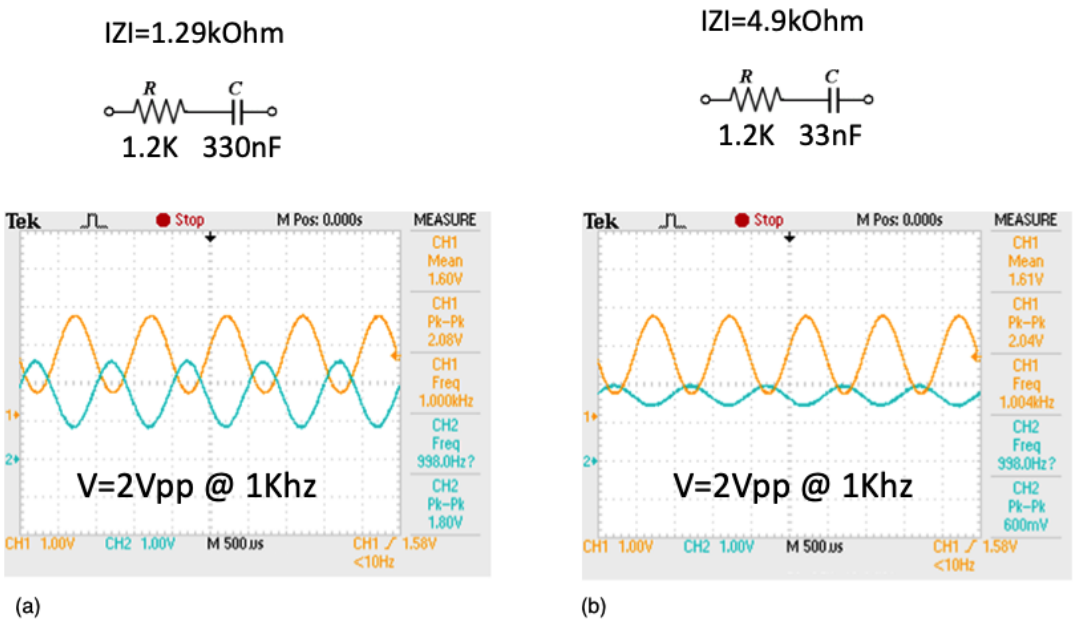

Figure 6.3: Oscilloscope outputs showing the signal of the output(orange)and the input voltage of AD5933 when the impedance Z= $Z_R + Z_C$ is (a) $|Z|$=1.29KΩ (b)$|Z|$=4.9KΩ

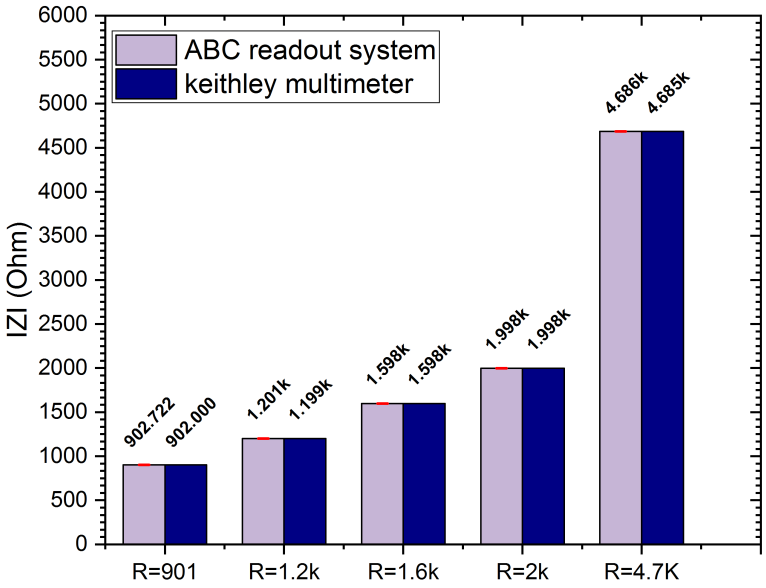

Figure 6.4: Plot showing different resistors values measured by ABC and compared to a commercial multimeter when Rcali is 1.2kOhm. Each measurement is repeated 200 times. Error bar indicates the standard deviation.

varies from 900 Ohm to 4.7 K Ohm using the ABC sensor. The results are compared against a commercial multimeter. Off shelf components (resistors and capacitors) of 1% tolerance are used. The calibration impedance remains 1.2 k Ohm.

Two hundred readings of each of the test impedance are considered. As shown in the figure 6.5, the error percentage is less than 0.5% of the tested complex impedance in our working measurement range. The error percentage is seen to increase as the tested impedance has higher magnitude than the calibration resistance. This can be explained by the increase of the thermal noise associated with the larger resistors.

6.3 Sample measurement

As this portable readout sensor is still in its developmental research phase, we referred to the data provided by our previous work [82] to test the efficiency of the impedance measurement. The microelectrodes used are SAW chips. In this test,Au-nanoparticles in liquid are used

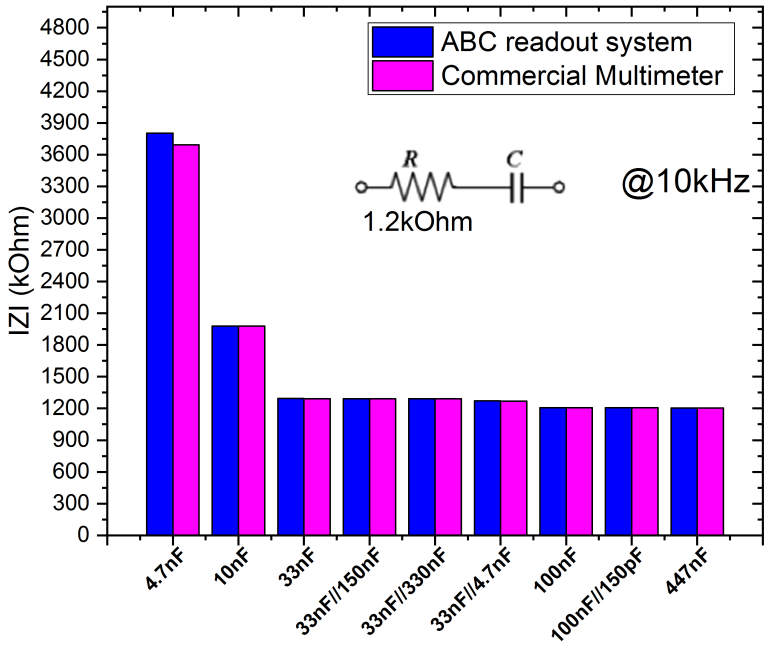

Figure 6.5: Plot showing complex values measured by ABC and compared to a commercial multimeter when Rcali is 1.2kOhm. Each measurement is repeated 200 times. Error bar indicates the standard deviation.

as the target to demonstrate the functionality of the ABC readout system. The excitation signal for this set of experiments is chosen to be 1 Vp-p sinusoidal signal at 10 kHz applied for 30 s. The control buffer is diluted phosphate-buffered saline (PBS) denoted as 0.1x PBS (15 mM Na+) This control sample is obtained by diluting 1:10 the solution 1x PBS with deionized water. Gold particles suspended in DI water are used in the detection experiments. Au-nanoparticles are of 20 nm in diameter and their received original stock is a 100 ppm (part per million) solution. A series of concentrations from 0.1 ppt to 100 ppt (part per trillion) are made by suspending nanoparticles in DI water. All the tested nanoparticles are purchased from Entegris, Inc. (Corporate Headquarters) in MA, USA. As the electrodes should be rigorously cleaned, the chips are soaked in acetone in a glass beaker on a stirrer for 15 min. Later, they are rinsed by isopropyl alcohol for 10 s and deionized water for another 10 s, and dried by an air gun. To make it hydrophilic, the electrode surface are treated by a UV ozone cleaner for 20 min. Then, the capacitance changes with time is recorded when 10μL of different concentrations of Au-nanoparticle solutions are applied onto the electrode surface.

Each concentration is tested in triplicate. Similarly to our previous work[82] and as shown in figure 6.6(a), for all the target samples, the normalized capacitance increases with time, indicating particle adsorption at the IDE surface. As the Au-nanoparticle concentration increases (the effective surface area of the sensor increases), larger capacitance increases are observed. The results plotted in figure correspond to the calculated mean of the normalized d$|C|$/dt (%/30s) values. The error bars represent the standard deviations of the repeated detection. As shown in the figure 6.6(b), the four nanoparticles samples and the background are clearly differentiated from each other. The responses are 0.8933± 0.18 %/30s 3.3688± 0.79 %/30s, 6.982± 0.49 %/30s and 6.9958± 1.01%/30s. The dose response is linear from 0.1 to 100 ppt and can be expressed as $Y = 0.965ln(x) + 3.3739$. where x is the target concentration . The d$|C|$/dt of the cut-off response is0.4125%/30s. This value is found by adding 3 standard deviations (30.0141%/30s) from the response of the background solution (-0.00105%/30s).

6.4 Multiplexed impedance sensing

After checking the hardware functionality of one channel detection, preliminary data are collected to check the efficiency of the multiplexed ACEK capacitive sensing . A fixed frequency test is conducted to measure the impedance change of a sensor over 30s. During this test, two saw chips are used to test the response of the buffer solution and 10 ppt of Au-nanoparticles samples. Initially, the MCU is programmed to test one channel impedance at a time, store the value in specific register then switch to the second channel and run the frequency sweep again to calculate the second sensor's impedance. By adopting this algorithm, One of the sensor however, channel 2 has a larger error percentage in measurement. It actually shows a mismatch from the expected impedance's values. This mismatch is due to the applied delay to measure channel one. Hence, the next alternative to program a more efficient algorithm is to switch between the channels while recording a single or very few measurements the selected channel.In deed, during the 30 seconds testing, the impedance analyzer samples the electrode impedance using the selected AC excitation signal for 5 times at an interval of 300 ns of each channel.

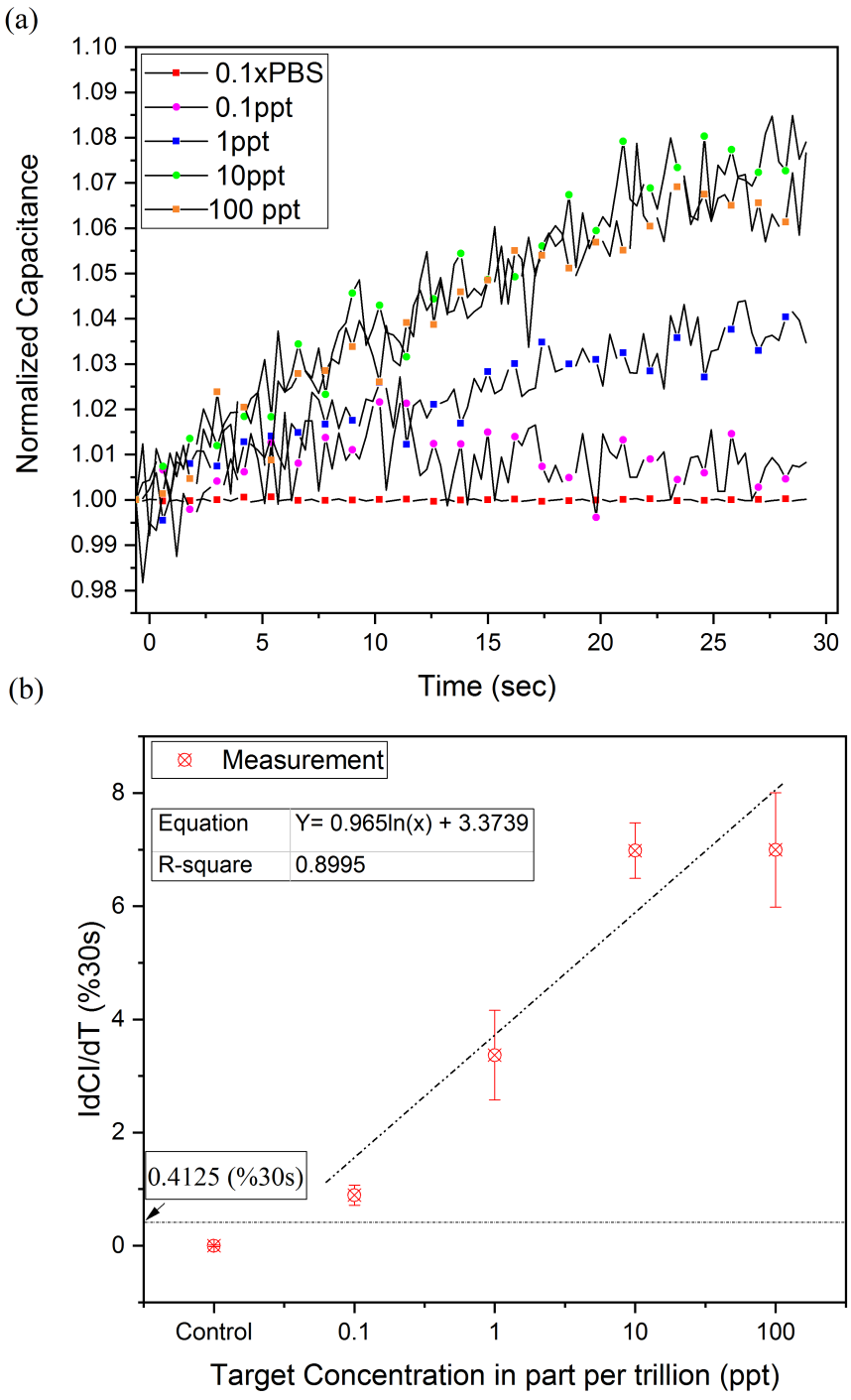

Figure 6.6: (a) Normalized capacitance change as a function of time within 30 seconds for different concentrations of Au-nanoparticle samples. An AC voltage of 1 Vp-p at 10 kHz is applied. (b) Dose response (capacitance change rates) from 4 different ofAu nanoparticle samples concentrations ranging from 0.1 to 100 ppt and the blank background control (0.1buffer. (b). the response value represents the average value of three measurements. the standard deviation is represented by the error bar in the plot. A linear fitting of the 4 different target response is also presented.

A delay of 0.3s is applied while switching between the channels. Besides, after every sample point, the MCU will read the data through serial inter-integrated circuit (I2C) interface to store the impedance values in two different arrays and then calculate the capacitance and its change rate of each channel. As shown in the figure 6.7, the system can measure the impedance. Although, the signal is more noisy while applying the multiplexed detection, the system shows a relatively good stability while recording impedance in our detection range.

6.5 Low voltage measurement

To be suitable for viral and bacterial DNA detection, the use of the AD5933 measurement chip should is extended to allow it to operate in low voltage configuration. In fact, most

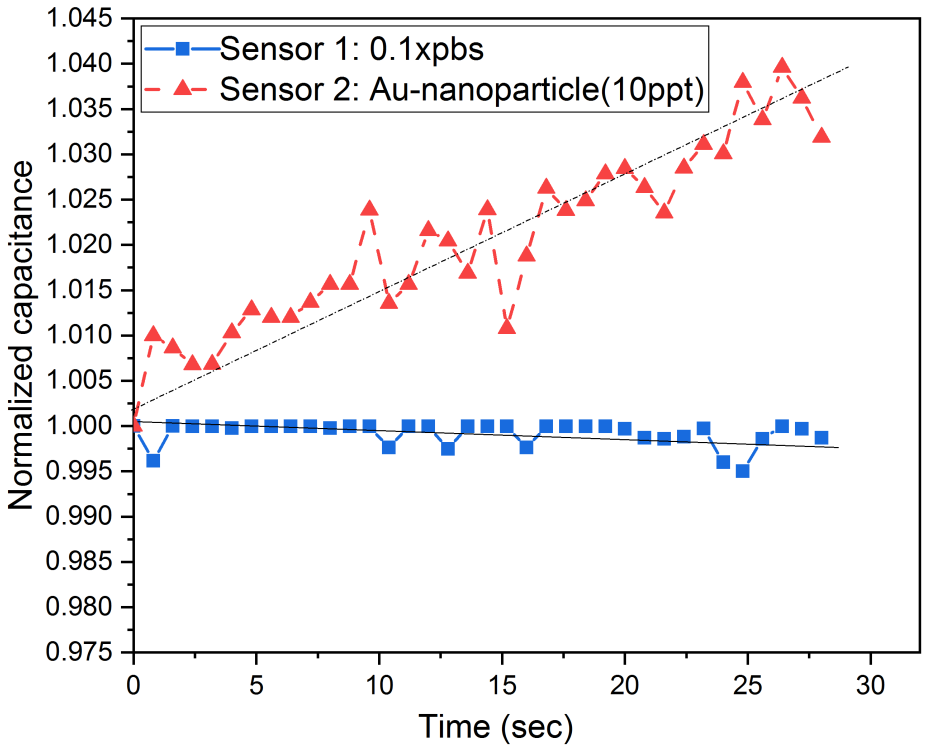

Figure 6.7: Normalized capacitance change as a function of time within 30 seconds for buffer solution and Au-nanoparticle samples. 1 Vp-p AC voltage is applied at 10 kHz .

of our DNA ACEK sensing protocols require a 10mVrms unbiased sinusoidal signal to be applied across the electrode for an optimal detection. However, AD5933 provides only four voltage ranges where the lowest is 200 mVpp. Hence, an extra circuitry is added to attenuate the excitation signal and filtered from any bias voltage before it can be applied to the sensor.

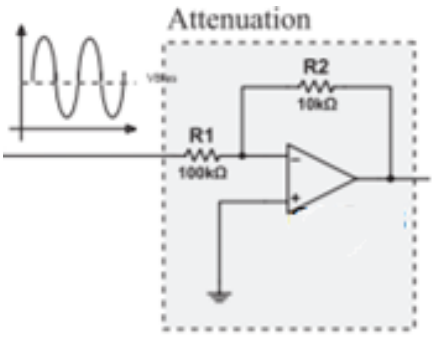

The attenuation stage is obtained by using a 1 channel operational amplifier AD8606 in an inverted configuration. The resistors R1 and R2 are controlling the gain of the used amplifier and the signal is attenuated by a factor of $R2/R1$. The key point is that the output impedance of the used amplifier (which is also in series with the tested sensor) has a far less significant effect on gain factor calibration and subsequent impedance readings in comparison to connecting the tested impedance directly to the Vout pin. As the average of our tested sensors impedance is relatively small (800ohm to 1.2 kohm), the external amplifier is chosen to have very low output resistance over the bandwidth of interest. ($\leq$ 1 Ω for Freq $\leq$100kHz and the gain Av=10).

With the values of R1 = 100 kΩ and R2 = 10 kΩ, attenuate the signal by 1/10th of 200 mV p-p = 20 mV. The maximum current flowing through the impedance is 20 mV/ 800Ω = 0.25 mA. The dynamic range of the input signal to the receiving side of the AD5933 can be improved by increasing the value of the I-V gain resistor at the RFB pin(see figure 6.8). This configuration helps to minimize the effect of the output resistance of AD5933 Vout pin. It also attenuates the peak-to-peak excitation voltage at the output of AD5933, ie, reduces the current flowing the tested impedance. Hence, with this configuration(figure 6.8) smaller impedance can be measured too without saturating the I-V amplifier in the receiving side of AD5933. Multiple resistors measurements are carried out to determine whether such a low voltage can keep the system accuracy and stability shown in the previous sections in this chapter. The system settings in this test are: VDD = 3.3 V VOUT = 200 mV p-p R2 = 10 kΩ R1 = 100 kΩ Gain setting resistor = 1.2 k Ω Measured Impedance= 800,1000, 1200 and 1600 Ω PGA setting = 1

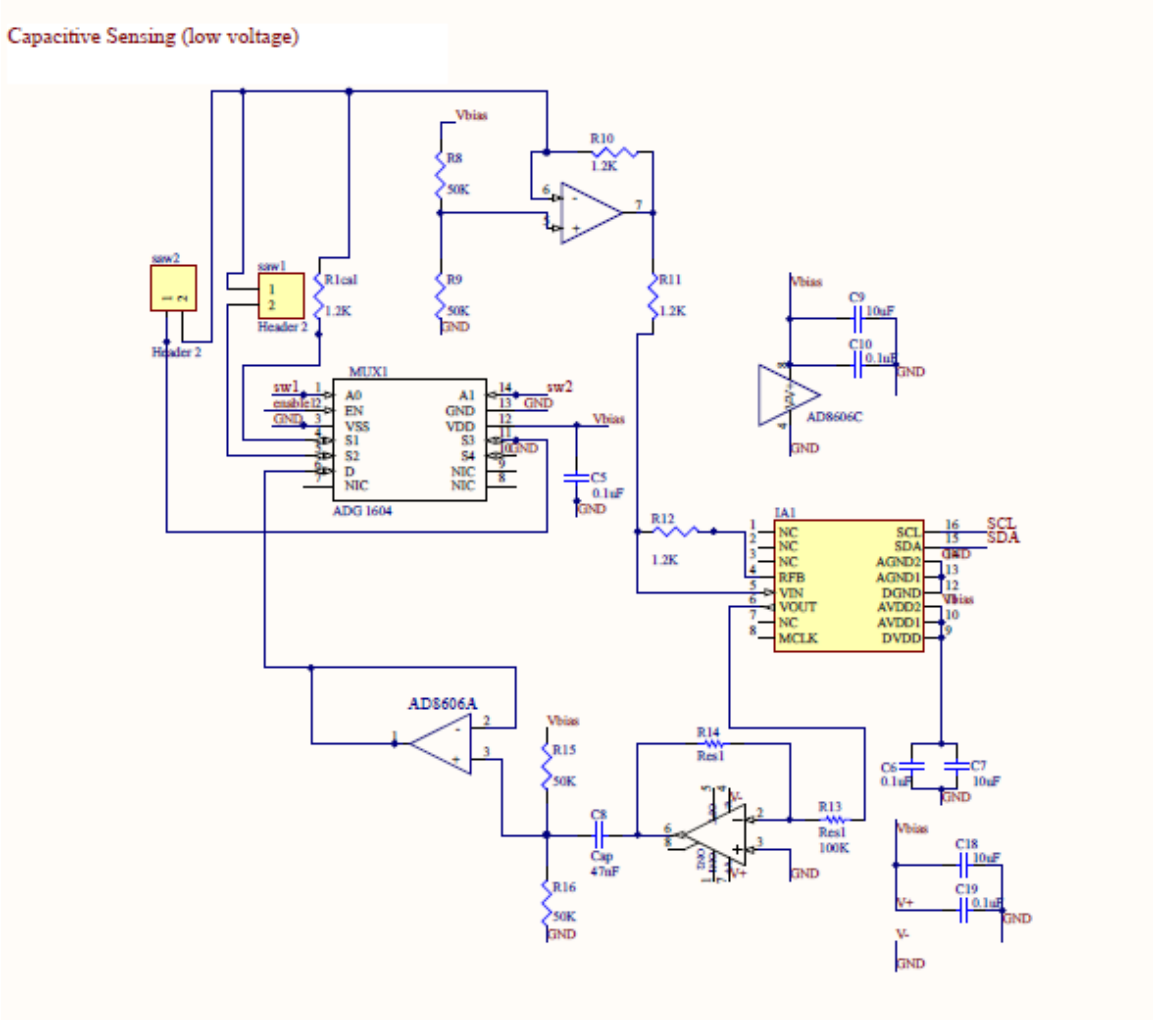

Figure 6.8: Low voltage capacitive sensing circuit

As shown in figure 6.9 the error of the impedance reading is 3% on average which is higher than the error in the multiplexed high voltage configuration (Figure 6.4).

This large error can be explained by a poor sampling of the impedance change by the ADC as by lowering the excitation voltage the dynamic range of the ADC shrinks. The dynamic range of the input signal to the receive side of the AD5933 can be improved by amplifying the response signal into the ADC(without exceeding 3.3 V to avoid saturation). The gain through the system (inside AD5933) shown in Figure 6.10 is given by [4]:

$$Gain = Excitationvoltage * \frac{Gainsettingresistor}{Measured - impedance} * PGA \tag{6.1}$$

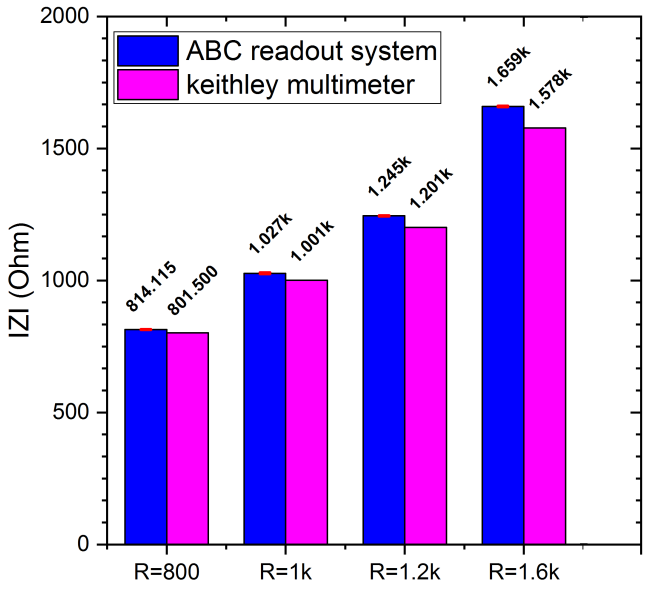

Figure 6.9: Plot showing different resistors values measured by ABC under low voltage configuration. The results are compared to a commercial multimeter when Rcali is 1.2kOhm. Each measurement is repeated 200 times.Error bar indicates the standard deviation.

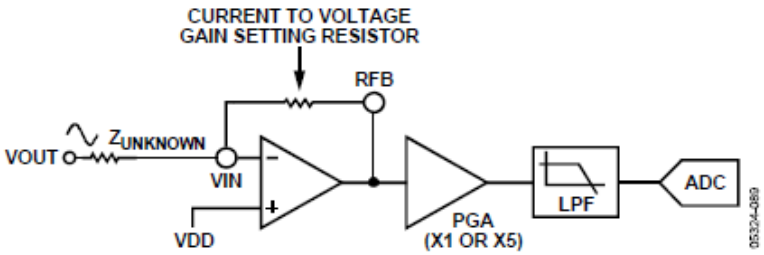

Figure 6.10: System Voltage Gain.[4]

Based on the equation 6.1, the safest and the easiest option to amplify the signal without saturating the ADC, is to program the PGA gain to be x5 instead of x1. So that the maximum voltage presented to the ADC will not exceed VDD=3.3V as long as the excitation voltage is less or equal than $200mV_{pp}$ (the peak-to-peak voltage presented to the ADC input will not exceed $200mV_{pp} * 5 = 1V_{pp}$).

Increasing the value of the I-V gain resistor at the RFB pin can be another solution to amplify the ADC input signal but this will add more hardware limitation to the circuit.

After building this software solution into the low voltage board, the system accuracy is improved and the reading errors are reduced to less than 0.2% in our DNA sensors impedance (from 800 to 1800 Ω)(see figure 6.11)

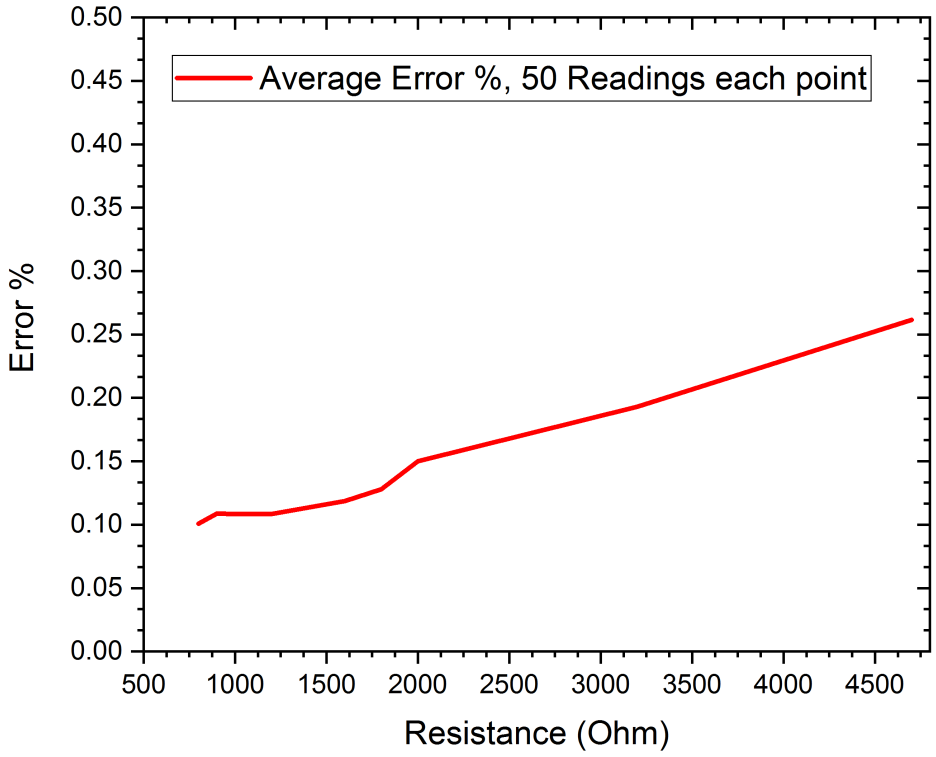

Figure 6.11: ABC measurement error percentage in low voltage configuration. the tested Impedance are from 800Ωto 5000Ω

Chapter 7

Conclusions

7.1 Conclusion

This work presents a low cost and a smart bio-diagnostic platform for point of care detection that can be used for bacterial DNAs and drug on-site detection. To achieve this goal, a development of assay protocols for highly sensitive and specific detection is required as well as a design of a portable readout system so a multiplexed on-site sensing can be reached. The achievements of this work include:

- Detection of cocaine from human serum. ACEO effect is used to speed up the transport of cocaine, which helps to develop a rapid, robust, lowcost and easy to use sensor. Without any signal amplification or use of label, the detection of cocaine molecules can be accomplished within 30 s. As discussed earlier, the developed sensor shows a linear detection range from 14.5 fM to 1.45 pM of cocaine with a limit of detection of 7.8 fM in PBS or 1.34 pM in neat serum. The use of Proteinase K helps to break down the proteins in the serum, and as a result, no purification is needed for testing serum samples. This ACEK capacitive aptasensor demonstrates very good sensitivity and specificity for serum-based detection, showing high potential to be implemented for on-site cocaine detection.

- By optimizing the probe concentration and assay time for the detection of hybridization, rapid, sensitive and specific detection of MRSA gDNA has been achieved using

a newly developed ABC biosensor. The sensor operation involves only heat treatment of double strains DNA (dsDNA), adding the sample to the electrode sensor, and then applying the specified AC signal for 10-30 sec. The LOD is calculated to be 4.72 DNA copies /L. The work will eventually lead to a rapid and PCR-free biosensor platform for on-site sensitive and specific detection of genetic sequences for a wide range of pathogens and biomaterials.

- A low cost and portable readout system based on AC electrokinetic capacitive sensing is presented. The designed platform costs ≈ $100 and each measurement costs less than $1. The device is built to interface with three electrochemical electrodes to measure their impedance change over time to evaluate specific detection. To test its accuracy and reliability, different resistors and capacitors values are tested to mimic the electrode equivalent model. Also, gold nanoparticles are adopted to test the multiplexed detection. To be suitable for bio impedance sensing as well as the induction of ACEK effects, an extended analog circuit is designed to condition the output excitation signal of the impedance analyzer. The conditioned signal is DC unbiased and attenuated so the readout system can generate sinusoids from amplitude 20 mV_{pp} to 2 V_{pp} and 1Hz to 100KHz frequency.

7.2 Future scope

Firstly, DNA and drugs samples are currently tested in two separate modules of the ABC board, where each module includes its own MCU and its own AD5933 chip. A desired prototype (see figure) for realizing one PCB board with one MCU and one AD5933 to detect DNA and drugs in the same time would be achieved by using relays/resistor bank to control the gain of the low voltage amplifier. Further Coding is needed to combine the two capacitive sensing modules.

Secondly, further improvement of the multiplexed testing can be achieved. As the detection of multiple analyte samples simultaneously is challenging and causes degradation in sensor performance, AI algorithms can be also implemented to predict the sensor response and hence minimize the effect of interference signal.

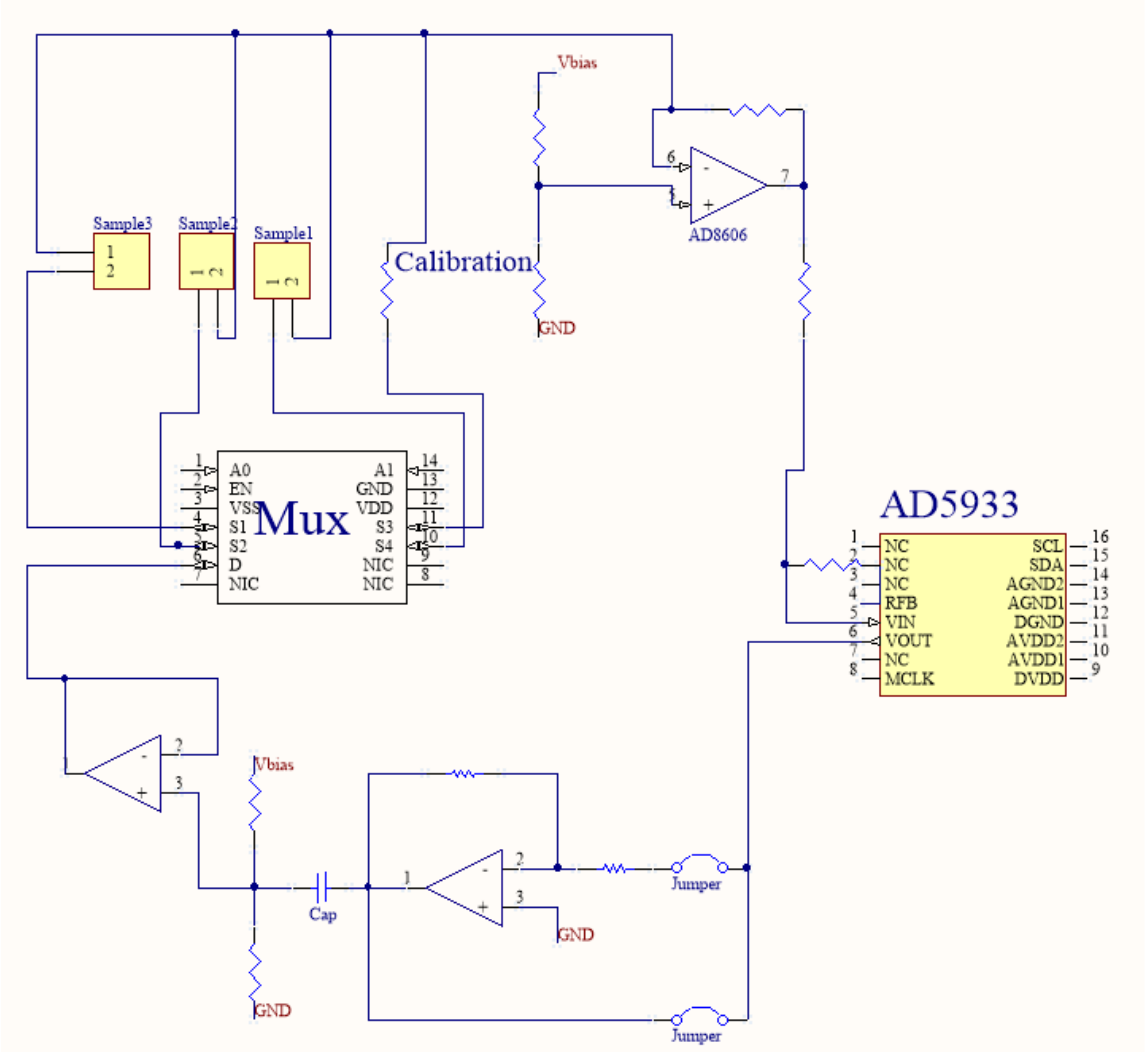

Figure 7.1: Proposed schematic of the Analog front end

Bibliography

[1] J. Jiang, X. Wang, R. Chao, Y. Ren, C. Hu, Z. Xu, and G. L. Liu, "Smartphone based portable bacteria pre-concentrating microfluidic sensor and impedance sensing system," *Sensors and Actuators B: Chemical*, vol. 193, pp. 653–659, 2014. 6, 20, 21, 22

[2] J. M. Sung, "Dielectrophoresis and optoelectronic tweezers for nanomanipulation," 2010. 6, 28

[3] J. Wu, "Interactions of electrical fields with fluids: laboratory-on-a-chip applications," *IET nanobiotechnology*, vol. 2, no. 1, pp. 14–27, 2008. 6, 14, 24, 27, 30, 31

[4] A. Devices, "Ad5933 datasheet," 2007. 9, 61, 62, 80, 81

[5] J. Fishovitz, J. A. Hermoso, M. Chang, and S. Mobashery, "Penicillin-binding protein 2a of methicillin-resistant staphylococcus aureus," *IUBMB life*, vol. 66, no. 8, pp. 572–577, 2014. 11, 18

[6] M. R. Pulido, M. García-Quintanilla, R. Martín-Peña, J. M. Cisneros, and M. J. McConnell, "Progress on the development of rapid methods for antimicrobial susceptibility testing," *Journal of Antimicrobial Chemotherapy*, vol. 68, no. 12, pp. 2710–2717, 2013. 11, 18

[7] J. Polisena, S. Chen, K. Cimon, S. McGill, K. Forward, and M. Gardam, "Clinical effectiveness of rapid tests for methicillin resistant staphylococcus aureus (mrsa) in hospitalized patients: a systematic review," *BMC Infectious Diseases*, vol. 11, no. 1, p. 336, 2011. 11, 18

[8] L. Karila, A. Petit, O. Phan, and M. Reynaud, "Cocaine induced psychotic disorders: a review," *Revue médicale de Liège*, vol. 65, no. 11, pp. 623–627, 2010. 11

[9] L. Degenhardt, W.-T. Chiu, N. Sampson, R. C. Kessler, J. C. Anthony, M. Angermeyer, R. Bruffaerts, G. De Girolamo, O. Gureje, Y. Huang *et al.*, "Toward a global view of alcohol, tobacco, cannabis, and cocaine use: findings from the who world mental health surveys," *PLoS medicine*, vol. 5, no. 7, p. e141, 2008. 11

[10] A. P. Turner, "Biosensors–sense and sensitivity," *Science*, vol. 290, no. 5495, pp. 1315–1317, 2000. 12

[11] F.-G. Banica, *Chemical sensors and biosensors: fundamentals and applications*. John Wiley & Sons, 2012. 12

[12] A. P. Turner, "Biosensors: sense and sensibility," *Chemical Society Reviews*, vol. 42, no. 8, pp. 3184–3196, 2013. 12

[13] L. Su, W. Jia, C. Hou, and Y. Lei, "Microbial biosensors: a review," *Biosensors and bioelectronics*, vol. 26, no. 5, pp. 1788–1799, 2011. 12

[14] A. Qureshi, Y. Gurbuz, and J. H. Niazi, "Biosensors for cardiac biomarkers detection: a review," *Sensors and Actuators B: Chemical*, vol. 171, pp. 62–76, 2012. 12

[15] K. Saha, S. S. Agasti, C. Kim, X. Li, and V. M. Rotello, "Gold nanoparticles in chemical and biological sensing," *Chemical reviews*, vol. 112, no. 5, pp. 2739–2779, 2012. 12

[16] Q. Liu, C. Wu, H. Cai, N. Hu, J. Zhou, and P. Wang, "Cell-based biosensors and their application in biomedicine," *Chemical reviews*, vol. 114, no. 12, pp. 6423–6461, 2014. 12, 37

[17] K. R. Rogers, "Principles of affinity-based biosensors," *Molecular biotechnology*, vol. 14, no. 2, pp. 109–129, 2000. 12

[18] J. S. Daniels and N. Pourmand, "Label-free impedance biosensors: Opportunities and challenges," *Electroanalysis*, vol. 19, no. 12, pp. 1239–1257, 2007. 12

[19] D. R. Thévenot, K. Toth, R. A. Durst, and G. S. Wilson, "Electrochemical biosensors: recommended definitions and classification," *Analytical Letters*, vol. 34, no. 5, pp. 635–659, 2001. 13

[20] T. G. Drummond, M. G. Hill, and J. K. Barton, "Electrochemical dna sensors," *Nature biotechnology*, vol. 21, no. 10, p. 1192, 2003. 13

[21] E. Bakker and M. Telting-Diaz, "Electrochemical sensors," *Analytical chemistry*, vol. 74, no. 12, pp. 2781–2800, 2002. 13

[22] C. I. Justino, T. A. Rocha-Santos, and A. C. Duarte, "Review of analytical figures of merit of sensors and biosensors in clinical applications," *TrAC Trends in Analytical Chemistry*, vol. 29, no. 10, pp. 1172–1183, 2010. 13

[23] J. H. Luong, K. B. Male, and J. D. Glennon, "Biosensor technology: technology push versus market pull," *Biotechnology advances*, vol. 26, no. 5, pp. 492–500, 2008. 13

[24] H. Cui, "Alternating current electrokinetics based capacitive affinity biosensor: A point-of-care diagnostic platform," 2015. 13

[25] X. Liu, K. Yang, A. Wadhwa, S. Eda, S. Li, and J. Wu, "Development of an ac electrokinetics-based immunoassay system for on-site serodiagnosis of infectious diseases," *Sensors and Actuators A: Physical*, vol. 171, no. 2, pp. 406–413, 2011. 14, 17, 27

[26] J. Wu, Y. Ben, and H.-C. Chang, "Particle detection by electrical impedance spectroscopy with asymmetric-polarization ac electroosmotic trapping," *Microfluidics and Nanofluidics*, vol. 1, no. 2, pp. 161–167, 2005. 14, 27, 29, 37

[27] C. Feng, S. Dai, and L. Wang, "Optical aptasensors for quantitative detection of small biomolecules: A review," *Biosensors and Bioelectronics*, vol. 59, pp. 64–74, 2014. 16

[28] B. Jiang, M. Wang, Y. Chen, J. Xie, and Y. Xiang, "Highly sensitive electrochemical detection of cocaine on graphene/aunp modified electrode via catalytic redox-recycling amplification," *Biosensors and Bioelectronics*, vol. 32, no. 1, pp. 305–308, 2012. 16, 17

[29] N. Hamaguchi, A. Ellington, and M. Stanton, "Aptamer beacons for the direct detection of proteins," *Analytical biochemistry*, vol. 294, no. 2, pp. 126–131, 2001. 16

[30] Y. Wen, H. Pei, Y. Wan, Y. Su, Q. Huang, S. Song, and C. Fan, "Dna nanostructure-decorated surfaces for enhanced aptamer-target binding and electrochemical cocaine sensors," *Analytical chemistry*, vol. 83, no. 19, pp. 7418–7423, 2011. 17

[31] A. Mokhtarzadeh, J. E. N. Dolatabadi, K. Abnous, M. de la Guardia, and M. Ramezani, "Nanomaterial-based cocaine aptasensors," *Biosensors and Bioelectronics*, vol. 68, pp. 95–106, 2015. 17

[32] T. Hermann and D. J. Patel, "Adaptive recognition by nucleic acid aptamers," *Science*, vol. 287, no. 5454, pp. 820–825, 2000. 17

[33] J. Zhang, L. Wang, D. Pan, S. Song, F. Y. Boey, H. Zhang, and C. Fan, "Visual cocaine detection with gold nanoparticles and rationally engineered aptamer structures," *small*, vol. 4, no. 8, pp. 1196–1200, 2008. 17

[34] A. D. Ellington and J. W. Szostak, "In vitro selection of rna molecules that bind specific ligands," *nature*, vol. 346, no. 6287, p. 818, 1990. 17

[35] Y. Li, X. Ji, and B. Liu, "Chemiluminescence aptasensor for cocaine based on double-functionalized gold nanoprobes and functionalized magnetic microbeads," *Analytical and bioanalytical chemistry*, vol. 401, no. 1, pp. 213–219, 2011. 17, 38

[36] M. Aires de Sousa and H. Lencastre de, "Bridges from hospitals to the laboratory: genetic portraits of methicillin-resistant staphylococcus aureus clones," *FEMS Immunology & Medical Microbiology*, vol. 40, no. 2, pp. 101–111, 2004. 18

[37] R. H. Deurenberg and E. E. Stobberingh, "The evolution of staphylococcus aureus," *Infection, genetics and evolution*, vol. 8, no. 6, pp. 747–763, 2008. 18

[38] G. K. Paterson, E. M. Harrison, and M. A. Holmes, "The emergence of mecc methicillin-resistant staphylococcus aureus," *Trends in microbiology*, vol. 22, no. 1, pp. 42–47, 2014. 18

[39] D. K. Corrigan, H. Schulze, G. Henihan, I. Ciani, G. Giraud, J. G. Terry, A. J. Walton, R. Pethig, P. Ghazal, J. Crain *et al.*, "Impedimetric detection of single-stranded pcr products derived from methicillin resistant staphylococcus aureus (mrsa) isolates," *Biosensors and Bioelectronics*, vol. 34, no. 1, pp. 178–184, 2012. 18, 19

[40] W. C. Lindsey, E. S. Woodruff, D. Weed, D. C. Ward, and R. D. Jenison, "Development of a rapid diagnostic assay for methicillin-resistant staphylococcus aureus and methicillin-resistant coagulase-negative staphylococcus," *Diagnostic microbiology and infectious disease*, vol. 61, no. 3, pp. 273–279, 2008. 18

[41] A. S. Rossney, C. M. Herra, G. I. Brennan, P. M. Morgan, and B. O'Connell, "Evaluation of the xpert methicillin-resistant staphylococcus aureus (mrsa) assay using the genexpert real-time pcr platform for rapid detection of mrsa from screening specimens," *Journal of clinical microbiology*, vol. 46, no. 10, pp. 3285–3290, 2008. 18

[42] T. Stenholm, A. J. Hakanen, J. Vaarno, S. Pihlasalo, P. Terho, P. E. Hänninen, J. Vuopio-Varkila, P. Huovinen, and P. Kotilainen, "Methicillin-resistant staphylococcus aureus screening by online immunometric monitoring of bacterial growth under selective pressure," *Antimicrobial agents and chemotherapy*, vol. 53, no. 12, pp. 5088–5094, 2009. 18

[43] S. Tombelli, M. Minunni, A. Santucci, M. Spiriti, and M. Mascini, "A dna-based piezoelectric biosensor: Strategies for coupling nucleic acids to piezoelectric devices," *Talanta*, vol. 68, no. 3, pp. 806–812, 2006. 19

[44] J. Hu, S. Wang, L. Wang, F. Li, B. Pingguan-Murphy, T. J. Lu, and F. Xu, "Advances in paper-based point-of-care diagnostics," *Biosensors and Bioelectronics*, vol. 54, pp. 585–597, 2014. 19

[45] O. Tokel, F. Inci, and U. Demirci, "Advances in plasmonic technologies for point of care applications," *Chemical reviews*, vol. 114, no. 11, pp. 5728–5752, 2014. 19

[46] S. Sang, Y. Wang, Q. Feng, Y. Wei, J. Ji, and W. Zhang, "Progress of new label-free techniques for biosensors: a review," *Critical reviews in biotechnology*, vol. 36, no. 3, pp. 465–481, 2016. 19

[47] K. N. Han, C. A. Li, and G. H. Seong, "Microfluidic chips for immunoassays," *Annual review of analytical chemistry*, vol. 6, pp. 119–141, 2013. 19

[48] S. Kumar, S. Kumar, M. A. Ali, P. Anand, V. V. Agrawal, R. John, S. Maji, and B. D. Malhotra, "Microfluidic-integrated biosensors: Prospects for point-of-care diagnostics," *Biotechnology journal*, vol. 8, no. 11, pp. 1267–1279, 2013. 19

[49] C. M. Li and W. Hu, "Electroanalysis in micro-and nano-scales," *Journal of Electroanalytical Chemistry*, vol. 688, pp. 20–31, 2013. 19

[50] R. L. Caygill, G. E. Blair, and P. A. Millner, "A review on viral biosensors to detect human pathogens," *Analytica Chimica Acta*, vol. 681, no. 1-2, pp. 8–15, 2010. 20

[51] R. Oueslati, C. Cheng, J. Wu, and J. Chen, "Highly sensitive and specific on-site detection of serum cocaine by a low cost aptasensor," *Biosensors and Bioelectronics*, vol. 108, pp. 103–108, 2018. 20

[52] J. Zhang, R. Oueslati, C. Cheng, L. Zhao, J. Chen, R. Almeida, and J. Wu, "Rapid, highly sensitive detection of gram-negative bacteria with lipopolysaccharide based disposable aptasensor," *Biosensors and Bioelectronics*, vol. 112, pp. 48–53, 2018. 20

[53] H. Mirzajani, C. Cheng, J. Wu, J. Chen, S. Eda, E. N. Aghdam, and H. B. Ghavifekr, "A highly sensitive and specific capacitive aptasensor for rapid and label-free trace analysis of bisphenol a (bpa) in canned foods," *Biosensors and Bioelectronics*, vol. 89, pp. 1059–1067, 2017. 20

[54] D. Zhang, Y. Lu, Q. Zhang, L. Liu, S. Li, Y. Yao, J. Jiang, G. L. Liu, and Q. Liu, "Protein detecting with smartphone-controlled electrochemical impedance spectroscopy for point-of-care applications," *Sensors and Actuators B: Chemical*, vol. 222, pp. 994–1002, 2016. 20, 22

[55] C.-H. Chuang, Y.-C. Yu, D.-H. Lee, T.-F. Wu, C.-H. Chen, S.-M. Chen, H.-P. Wu, and Y.-W. Huang, "Miniaturization of immunoassay by using a novel module-level immunosensor with polyaniline-modified nanoprobes that incorporate impedance sensing and paper-based sampling," *Microfluidics and nanofluidics*, vol. 16, no. 5, pp. 869–877, 2014. 20, 22

[56] M. Grossi, M. Lanzoni, A. Pompei, R. Lazzarini, D. Matteuzzi, and B. Riccò, "An embedded portable biosensor system for bacterial concentration detection," *Biosensors and Bioelectronics*, vol. 26, no. 3, pp. 983–990, 2010. 20

[57] D. Zhang, J. Jiang, J. Chen, Q. Zhang, Y. Lu, Y. Yao, S. Li, G. L. Liu, and Q. Liu, "Smartphone-based portable biosensing system using impedance measurement

with printed electrodes for 2, 4, 6-trinitrotoluene (tnt) detection," *Biosensors and Bioelectronics*, vol. 70, pp. 81–88, 2015. 22

[58] H. Cui, J. Wu, S. Eda, J. Chen, W. Chen, and L. Zheng, "Rapid capacitive detection of femtomolar levels of bisphenol a using an aptamer-modified disposable microelectrode array," *Microchimica Acta*, vol. 182, no. 13-14, pp. 2361–2367, 2015. 24

[59] X. Liu, C. Cheng, J. Wu, S. Eda, and Y. Guo, "A low cost and palm-size analyzer for rapid and sensitive protein detection by ac electrokinetics capacitive sensing," *Biosensors and Bioelectronics*, vol. 90, pp. 83–90, 2017. 24

[60] C. Cheng, H. Cui, J. Wu, and S. Eda, "A pcr-free point-of-care capacitive immunoassay for influenza a virus," *Microchimica Acta*, vol. 184, no. 6, pp. 1649–1657, 2017. 24

[61] C. Cheng, R. Oueslati, J. Wu, J. Chen, and S. Eda, "Capacitive dna sensor for rapid and sensitive detection of whole genome human herpesvirus-1 dsdna in serum," *Electrophoresis*, vol. 38, no. 12, pp. 1617–1623, 2017. 24, 29, 40, 49

[62] E. Barsoukov and J. R. Macdonald, *Impedance spectroscopy: theory, experiment, and applications*. John Wiley & Sons, 2018. 24

[63] H. Cui, S. Li, Q. Yuan, A. Wadhwa, S. Eda, M. Chambers, R. Ashford, H. Jiang, and J. Wu, "An ac electrokinetic impedance immunosensor for rapid detection of tuberculosis," *Analyst*, vol. 138, no. 23, pp. 7188–7196, 2013. 24

[64] C. Cheng, S. Wang, J. Wu, Y. Yu, R. Li, S. Eda, J. Chen, G. Feng, B. Lawrie, and A. Hu, "Bisphenol a sensors on polyimide fabricated by laser direct writing for onsite river water monitoring at attomolar concentration," *ACS applied materials & interfaces*, vol. 8, no. 28, pp. 17 784–17 792, 2016. 24, 37, 39

[65] P. E. Sheehan and L. J. Whitman, "Detection limits for nanoscale biosensors," *Nano letters*, vol. 5, no. 4, pp. 803–807, 2005. 27

[66] A. Castellanos, A. Ramos, A. Gonzalez, N. G. Green, and H. Morgan, "Electrohydrodynamics and dielectrophoresis in microsystems: scaling laws," *Journal of Physics D: Applied Physics*, vol. 36, no. 20, p. 2584, 2003. 27, 30, 37

[67] A. Lenshof and T. Laurell, "Continuous separation of cells and particles in microfluidic systems," *Chemical Society Reviews*, vol. 39, no. 3, pp. 1203–1217, 2010. 27

[68] S. Li, Q. Yuan, B. I. Morshed, C. Ke, J. Wu, and H. Jiang, "Dielectrophoretic responses of dna and fluorophore in physiological solution by impedimetric characterization," *Biosensors and Bioelectronics*, vol. 41, pp. 649–655, 2013. 27

[69] C. Páez-Avilés, E. Juanola-Feliu, J. Punter-Villagrasa, B. del Moral Zamora, A. Homs-Corbera, J. Colomer-Farrarons, P. Miribel-Català, and J. Samitier, "Combined dielectrophoresis and impedance systems for bacteria analysis in microfluidic on-chip platforms," *Sensors*, vol. 16, no. 9, p. 1514, 2016. 27

[70] Y. Demircan, E. Özgür, and H. Külah, "Dielectrophoresis: Applications and future outlook in point of care," *Electrophoresis*, vol. 34, no. 7, pp. 1008–1027, 2013. 27

[71] R. Pethig, "Dielectrophoresis: Status of the theory, technology, and applications," *Biomicrofluidics*, vol. 4, no. 2, p. 022811, 2010. 27

[72] N. G. Green, A. Ramos, A. González, H. Morgan, and A. Castellanos, "Fluid flow induced by nonuniform ac electric fields in electrolytes on microelectrodes. i. experimental measurements," *Physical review E*, vol. 61, no. 4, p. 4011, 2000. 29

[73] A. Ramos, H. Morgan, N. G. Green, and A. Castellanos, "Ac electrokinetics: a review of forces in microelectrode structures," *Journal of Physics D: Applied Physics*, vol. 31, no. 18, p. 2338, 1998. 29

[74] H. Cui, C. Cheng, J. Wu, and S. Eda, "Rapid detection of progesterone by commercially available microelectrode chips," in *SENSORS, 2013 IEEE*. IEEE, 2013, pp. 1–4. 33

[75] K. Yang and J. Wu, "Investigation of microflow reversal by ac electrokinetics in orthogonal electrodes for micropump design," *Biomicrofluidics*, vol. 2, no. 2, p. 024101, 2008. 37

[76] S. Li, Y. Ren, H. Cui, Q. Yuan, J. Wu, S. Eda, and H. Jiang, "Alternating current electrokinetics enhanced in situ capacitive immunoassay," *Electrophoresis*, vol. 36, no. 3, pp. 471–474, 2015. 39

[77] M. Maurizi, "Proteases and protein degradation inescherichia coli," *Experientia*, vol. 48, no. 2, pp. 178–201, 1992. 42

[78] D. Jonas, M. Speck, F. Daschner, and H. Grundmann, "Rapid pcr-based identification of methicillin-resistant staphylococcus aureus from screening swabs," *Journal of Clinical Microbiology*, vol. 40, no. 5, pp. 1821–1823, 2002. 45, 53

[79] M. Minunni, S. Tombelli, R. Scielzi, I. Mannelli, M. Mascini, and C. Gaudiano, "Detection of β-thalassemia by a dna piezoelectric biosensor coupled with polymerase chain reaction," *Analytica chimica acta*, vol. 481, no. 1, pp. 55–64, 2003. 45

[80] S. Li, H. Cui, Q. Yuan, J. Wu, A. Wadhwa, S. Eda, and H. Jiang, "Ac electrokinetics-enhanced capacitive immunosensor for point-of-care serodiagnosis of infectious diseases," *Biosensors and Bioelectronics*, vol. 51, pp. 437–443, 2014. 45, 50

[81] H. Cui, C. Cheng, X. Lin, J. Wu, J. Chen, S. Eda, and Q. Yuan, "Rapid and sensitive detection of small biomolecule by capacitive sensing and low field ac electrothermal effect," *Sensors and Actuators B: Chemical*, vol. 226, pp. 245–253, 2016. 45, 48, 50

[82] J. Zhang, J. Wang, J. Wu, H. Qi, C. Wang, X. Fang, C. Cheng, and W. Yang, "Rapid detection of ultra-trace nanoparticles based on acek enrichment for semiconductor manufacturing quality control," *Microfluidics and Nanofluidics*, vol. 23, no. 1, p. 2, 2019. 48, 73, 75

[83] D. Jonas, H. Grundmann, D. Hartung, F. Daschner, and K. Towner, "Evaluation of the meca femb duplex polymerase chain reaction for detection of methicillin-resistant staphylococcus aureus," *European Journal of Clinical Microbiology and Infectious Diseases*, vol. 18, no. 9, pp. 643–647, 1999. 53

[84] S. Grimnes and O. Martinsen, "Bioimpedance and bioelectricity basics academic press," *New York*, 2000. 61

Appendix

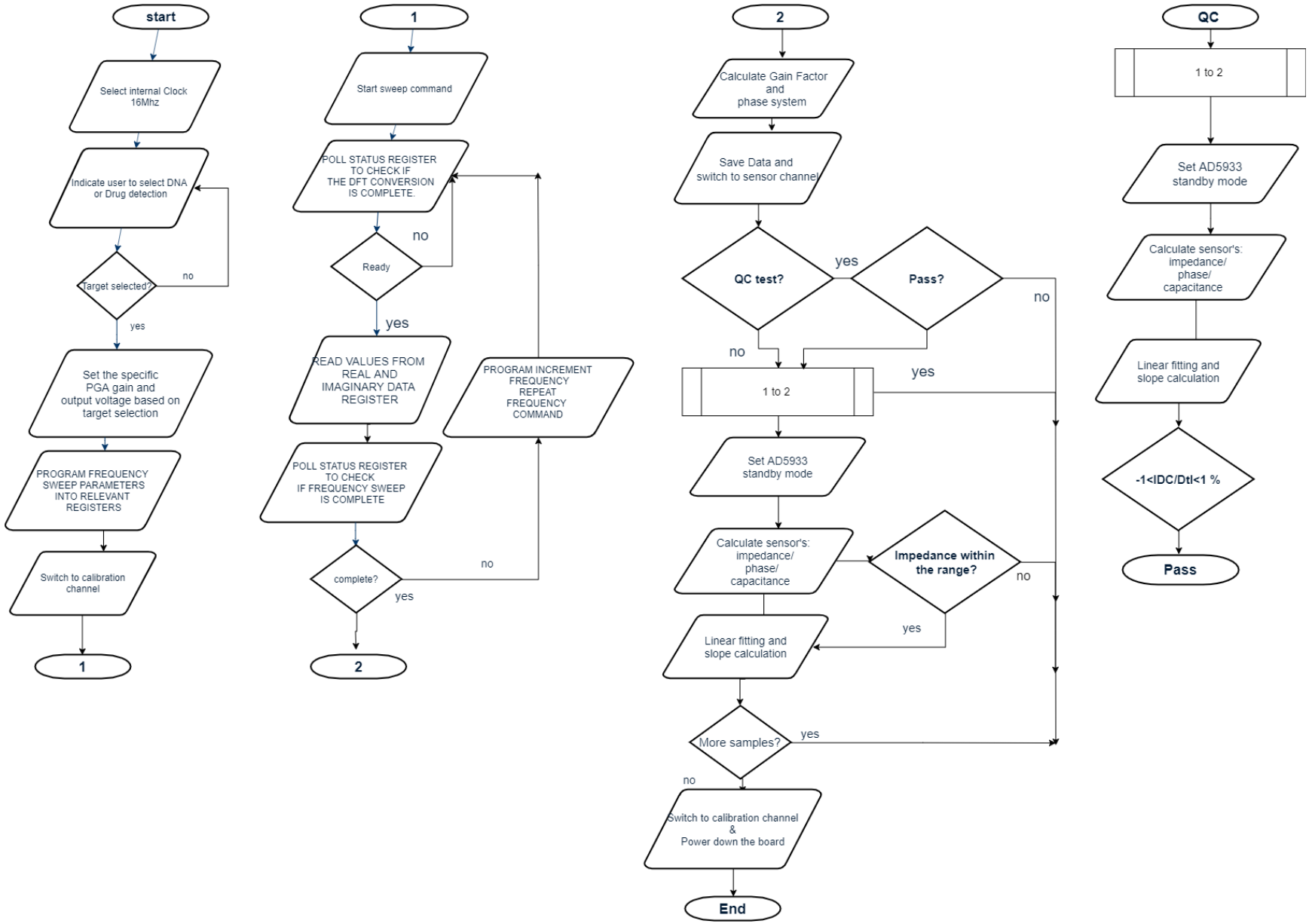

Figure 7.2: Flowchart of the ABC measurement program.

Vita

Rania Oueslati received the B.S. and M.S. degrees in electrical engineering from the University of Tunis, Tunisia. She is currently studying on her PhD program at the Department of Electrical Engineering and Computer Science, University of Tennessee, Knoxville. In 2015, she was an exchange scholar in Imaging, Robotics, and Intelligent Systems (IRIS) Laboratory at university of Tennessee Knoxville. Her research interest included the development of hybrid and embedded systems for image processing. Since 2016, she has been a research assistant in Dr. Wus group. Her research interests include biosensor and bio-detection, lab on one chip system and micro-fluidic system based on AC electrokinetic. **She is the author of seven conference papers and four peer reviewed journal articles (one is accepted with major revision)**. Rania ′s award and honors include Grace Hopper Student Scholarship, the Advancing Electrokinetic Science (AES) award (Funded by NSF) and Chancellors Citation Award for Extraordinary Professional Promise.